

## General Disclaimer

### One or more of the Following Statements may affect this Document

- This document has been reproduced from the best copy furnished by the organizational source. It is being released in the interest of making available as much information as possible.
- This document may contain data, which exceeds the sheet parameters. It was furnished in this condition by the organizational source and is the best copy available.
- This document may contain tone-on-tone or color graphs, charts and/or pictures, which have been reproduced in black and white.
- This document is paginated as submitted by the original source.
- Portions of this document are not fully legible due to the historical nature of some of the material. However, it is the best reproduction available from the original submission.

## Conceptual Design for Spacelab Pool Boiling Experiment

J. H. Lienhard  
R. E. Peck

Boiling and Phase  
Change Laboratory  
Department of  
Mechanical Engineering

NASA CR-135378  
UKY TR106-78-ME15

Prepared for:  
National Aeronautics and Space Administration  
Lewis Research Center  
21000 Brookpark Road  
Cleveland, Ohio 44135  
Contract NAS3-20397

Prepared by:  
Office of Research and Engineering Services  
College of Engineering  
University of Kentucky  
Lexington, Kentucky 40506



1. Report No. NASA CR-135378		2. Government Accession No.		3. Recipient's Catalog No.	
4. Title and Subtitle Conceptual Design for Spacelab Pool Boiling Experiment				5. Report Date March 1978	
				6. Performing Organization Code	
7. Author(s) John H. Lienhard and Robert E. Peck				8. Performing Organization Report No. UKY TR106-78-ME15	
9. Performing Organization Name and Address Boiling and Phase Change Laboratory Mechanical Engineering Department University of Kentucky Lexington, Kentucky 40506				10. Work Unit No.	
				11. Contract or Grant No. NAS3-20397	
				13. Type of Report and Period Covered Contractor Report	
12. Sponsoring Agency Name and Address National Aeronautics and Space Administration Washington, D.C. 20546				14. Sponsoring Agency Code	
15. Supplementary Notes Project Manager, Thomas H. Cochran, Space Propulsion and Power Division NASA Lewis Research Center, Cleveland, Ohio 44135					
16. Abstract A relatively small, and very simple, basic research experiment in pool boiling heat transfer is designed to be incorporated with a larger two-phase flow experiment being designed by the General Dynamics Convair Division. The experiment is intended to confirm (or alter) the results of earth-normal gravity experiments which indicate that the hydrodynamic peak and minimum pool boiling heat fluxes vanish at very low gravity. Twelve small sealed test cells containing water, methanol or Freon 113 and cylindrical heaters of various sizes are to be built. Each cell will be subjected to one or more 45 sec tests in which the surface heat flux on the heaters is increased linearly until the surface temperature reaches a limiting value of 500°C. The entire boiling process will be photographed in slow-motion. Boiling curves will be constructed from thermocouple and electric input data, for comparison with the motion picture records. The conduct of the experiment will require no more than a few hours of operator time.					
17. Key Words (Suggested by Author(s)) Pool Boiling Peak Boiling Heat Flux Reduced Gravity Spacelab Manned Orbital Research Laboratories-				18. Distribution Statement Unclassified Unlimited	
19. Security Classif. (of this report) Unclassified		20. Security Classif. (of this page) Unclassified		21. No. of Pages 84	22. Price*

## FOREWORD

The pool boiling experiment developed herein was motivated by preliminary experiments and rationale done by Nanik Bakhru as his doctoral dissertation under the direction of John H. Lienhard at the University of Kentucky and under the support of an earlier NASA research grant (NGR18-001-035). This conceptual design study was done under NASA Contract NAS3-20397 in the Boiling and Phase Change Laboratory of the University of Kentucky's Mechanical Engineering Department. Mr. Thomas H. Cochran served as Project Manager both for this Contract and the antecedent Grant. His contributions to the success of both were varied, unselfish, and substantial.

The Principal Investigator in this work was Professor John H. Lienhard. He and Professor Robert E. Peck of the University of Kentucky co-authored this report. Dr. R. Bhatti also worked on the contract in its early stages, and developed much of the material in section II-C. This experiment is eventually to be incorporated into the much larger Flow Boiling experiment being designed by R.D. Bradshaw and C.D. King of General Dynamics Convair Division under NASA Contract NAS3-20389. Their design reports have also been very helpful in the present work.

TABLE OF CONTENTS

	<u>Page</u>
LIST OF FIGURES	vii
LIST OF TABLES	ix
SUMMARY	xi
TASK I: SCIENTIFIC JUSTIFICATION	1
TASK II: CONCEPTUAL DESIGN OF EXPERIMENTS	5
A. Objectives	5
B. Approach	6
Geometrical considerations	6
Independent variables	6
Experimental technique	7
C. Liquid Selection and Sizing of Heaters	8
Physical properties	10
Selection	11
The flickering phenomenon	24
Thermal capacity	27
D. Heat Flux Predictions	27
E. Mechanical Design	28
The test heaters	28
The heater power	38
The test cells	40
The heat rejection problem	42
The cell preheater	45
The cell pressure	46
Preflight test cells preparation	46
F. Supporting Requirements	48
Environmental	48
Volume and Weight	49
G. Procedure	49
H. Data Acquisition	50
I. Cost Analysis	53
J. An Alternate Experimental Arrangement	54
REFERENCES	55
APPENDIX A	57

LIST OF FIGURES

<u>Figure</u>		<u>Page</u>
1	Schematic diagram of the spacelab pool boiling experiment.	9
2a	Variation of heater radius with pressure for $R' = 0.005$ and $\frac{g}{g_e} = 10^{-4}$ .	16
2b	Variation of heater radius with pressure for $R' = 0.005$ and $\frac{g}{g_e} = 10^{-2}$ .	17
2c	Variation of heater radius with pressure for $R' = 0.03$ and $\frac{g}{g_e} = 10^{-4}$ .	18
2d	Variation of heater radius with pressure for $R' = 0.03$ and $\frac{g}{g_e} = 10^{-2}$ .	19
2e	Variation of heater radius with pressure for $R' = 0.2$ and $\frac{g}{g_e} = 10^{-4}$ .	20
2f	Variation of heater radius with pressure for $R' = 0.2$ and $\frac{g}{g_e} = 10^{-2}$ .	21
3	Dependence of the flickering parameter on system variables.	26
4a	Predicted heat removal from a 0.1524 cm cylindrical platinum heater in water: $p_{sat} = 0.17 \text{ atm}$ , $T_{sat} = 57^\circ\text{C}$ .	29
4b	Predicted heat removal from a 0.0254 cm cylindrical platinum heater in water: $p_{sat} = 0.17$ , $T_{sat} = 57^\circ\text{C}$ .	30
4c	Predicted heat removal from a 0.635 cm cylindrical platinum heater in methanol: $p_{sat} = 0.33 \text{ atm}$ , $T_{sat} = 39^\circ\text{C}$ .	31
4d	Predicted heat removal from a 0.17 cm cylindrical platinum heater in methanol: $p_{sat} = 0.33 \text{ atm}$ , $T_{sat} = 39^\circ\text{C}$ .	32
4e	Predicted heat removal from a 0.061 cm cylindrical platinum heater in Freon 113: $p_{sat} = 0.67 \text{ atm}$ , $T_{sat} = 36^\circ\text{C}$ .	33
4f	Predicted heat removal from a 0.61 cm cylindrical platinum heater in Freon 113: $p_{sat} = 0.67 \text{ atm}$ , $T_{sat} = 36^\circ\text{C}$ .	34

LIST OF FIGURES (Continued)

Figure		Page
5	The configuration of the heater rods with six thermocouples in each one.	36
6	Installation of the test heaters in the box.	37
7	Test cell configurations.	41
8	Method of window retention.	43
9	A vapor patch propagation sequence illustrating propagation of a vapor front, 0.0254 mm pt. wire. $R' = .016$ , $q = 520,000 \text{ W/m}^2$ (after Bakhru).	52

LIST OF TABLES

<u>Table</u>		<u>Page</u>
1	Properties of Saturated Liquids at a Pressure of 1 atm or 101,300 Newtons per Square Meter	12
2	Properties of Saturated Liquids at a Pressure of 0.6684 atm or 67,730 Newtons per Square Meter	13
3	Properties of Saturated Liquids at a Pressure of 0.3342 atm or 33,860 Newtons per Square Meter	14
4	Properties of Saturated Liquids at a Pressure of 0.0668 atm or 6,773 Newtons per Square Meter	15
5	Heater Size and Power Requirements	39
6	Temperature Rise Calculation	44
7	Preheater Power Requirements	47



SUMMARY

A simple experiment is formulated to facilitate the study of pool boiling in the low gravity environments of the spacelab. The experiment is contrived in such a way as to corroborate (or correct) and extend the scope of Bakhru's earth-normal gravity experiments. Bakhru's work showed, through the use of proven scaling laws, that the hydrodynamically determined peak and minimum heat fluxes would cease to occur at low enough gravity. He also noted many features of the character of boiling at low gravity. The experiment will investigate these characteristics under the conditions for which they were predicted.

The apparatus will consist of a set of small, sealed test cells, each containing a single cylindrical platinum electric heating element immersed in liquid water, methanol, or Freon-113. Various combinations of fluid properties, heater diameter, and g-level ( $10^{-2}$  and  $10^{-4} g_{\text{earth}}$ ) will provide information over a range of twelve test conditions.

The experimental procedure will require preconditioning the cells to the prescribed saturation temperature. An independent battery power supply to the heater will then be linearly increased for 45 seconds or until the heater temperature exceeds  $500^{\circ}\text{C}$ . It has been verified that the test conditions in the cell will remain nearly constant during this brief test period.

The cylinder heat flux and temperature and the cell temperature and pressure will be continuously recorded during the run in conjunction with high-speed filming of the boiling process. The total time needed to complete all of the twelve tests is estimated

to be about two hours. The data will be used to construct complete boiling curves for each set of test parameters. The photographic data will show the nature of vapor removal and the motion of vapor patches, once boiling has begun.

The experimental system is designed to be operated within the two-phase flow experiments being designed by General Dynamics Corvair Division. The weight of the experiment package will be about 60 kg. The estimated preflight cost of the experiment is \$46,500.

TASK I: SCIENTIFIC JUSTIFICATION

A problem that has long vexed NASA (see, e.g., an early review by Siegel [1]<sup>1</sup>) is that of understanding what the limit of nucleate boiling will be in reduced gravity. Siegel was one of the first people who devoted serious attention to low-gravity phenomena and one of his main concerns was determining the influence of gravity on the peak heat flux,  $q_{\max}$ . Reference [1] refers to many studies of low gravity burnout which, like the pioneering high-gravity studies of Costello (see, e.g., [2]), sought to validate or disprove the one-fourth power dependency of  $q_{\max}$  on gravity,  $g$ , that the Zuber-Kutateladze hydrodynamic theory [3] predicted.

These studies generally showed that the one-fourth power law was shaky at best. Costello, who pointed to this shakiness in expressing his doubts about the hydrodynamic theory in the early 1960's, was just starting to perceive the real reason for the failure of Zuber's theory at the time of his premature death in 1965 [4]. The reason was that Zuber's theory was being erroneously applied to finite heaters of all shapes, when it had only been derived for an infinite, horizontal, upward-facing heater.

In 1968, Lienhard [5] showed formally that Costello and Adams' idea was correct -- that in a finite heater configuration, the influence of gravity entered, not only as  $g^{1/4}$  in Zuber's flat plate expression, but also through a geometrical function of  $R'$  where:

$$R' \equiv R \sqrt{g(\rho_f - \rho_g) / \sigma} \quad (1)$$

---

<sup>1</sup>Numbers in square brackets denote entries in REFERENCES.

in which  $\rho_f$  and  $\rho_g$  are the saturated liquid and vapor densities, and  $\sigma$  is the surface tension, all evaluated at the local saturation temperature,  $T_{sat}$ .

NASA was interested in this discovery and, in 1967, they funded an extended program at the University of Kentucky Boiling and Phase-Change Laboratory to explore it fully. By 1973 this program had produced an extensive study of interacting geometrical and gravity effects which is summarized in the NASA contractor reports: [6,7]. This work resulted in a complete hydrodynamic theory of the peak and minimum pool boiling heat fluxes for large classes of finite heaters. The influence of viscosity, the electrolysis analogue, related questions of the influence of induced convection in certain configurations, were among the many factors considered in the effort.

But the key issue in this exploration was that of determining how  $q_{max}$  behaved as  $g$  approached zero. A number of specific predictions for  $q_{max}$  were developed for different configurations. They all took the form

$$\frac{q_{max}}{q_{max,Zuber}} = fn(R') \quad (2)$$

These expressions were highly successful but they failed to correlate data for  $R'$  on the order of 0.1 or less. This failure was entirely understandable since  $R'$  is the square root of the ratio of gravity to capillary forces. When  $R'$  is below 0.1, gravity is swamped by surface tension, and the hydrodynamic mechanisms (which depend upon the balancing of both forces) can no longer take place.

This result placed the study -- and NASA -- in an awkward position. If hydrodynamic "burnout" no longer occurred at low gravity, then what did? Siegel and others had observed some sort of change of behavior

that they might have viewed as a hydrodynamic transition. The literature was shot through with the idea that there was a peak heat flux at a low gravity. The final step in the NASA study was therefore to study  $q_{\max}$  closely at very small values of  $R'$ .

To make observations at small values of  $R'$  one must either make extended studies in a low-gravity environment or obtain data on extremely small wires at earth normal gravity. Only the latter course was then open, and Bakhru [8] undertook to develop such an experiment. The result of his effort was the basic paper which demonstrated the need for the present space shuttle experiment. Because of its importance we include it in its entirety in Appendix A. The key ideas from this paper are:

- 1) The visual details of boiling when  $R'$  is on the order of 0.01 show a complete absence of the hydrodynamic processes.
- 2) Plots of the wall superheat against the heat flux,  $q$ , from the wire, show that the conventional multivalued behavior vanishes as  $R'$  decreases and the curves are entirely monotonic when  $R'$  is on the order of 0.01.
- 3) There is no nucleate boiling in the range:  $R' < 0.01$ . Instead the wire is blanketed with patches of film boiling. Under some conditions the patches grow and collapse (or "flicker") and under others they are stationary. In either case the fraction of the wire that is blanketed increases with heat flux until blanketing is complete.
- 4) Whether the vapor patches flicker or remain stationary depends on the magnitude of a "flickering parameter",  $\Lambda$ , where<sup>2</sup>:

<sup>2</sup>Symbols not defined in context are explained in the nomenclature section of the paper in Appendix A.

$$\Lambda \equiv 2\sigma h_{fg} T_{sat} / k h_{fg} \Delta T \quad (3)$$

In water, for which  $\Lambda$  was about 0.17, the vapor patches flickered on and off. In the organic fluids,  $\Lambda$  was always less than about 0.02 and flickering never occurred.

TASK II: CONCEPTUAL DESIGN OF EXPERIMENTSA. Objectives

Bakhru's work makes it absolutely clear that, under low gravity there should be radical changes from conventional boiling behavior. The hydrodynamic mechanisms cease to exist and are replaced by something different.

The problem is that modeling low gravity conditions with small wires might possibly give a wrong impression of the nature of the replacement phenomenon. Not only did Bakhru's wires have very low thermal capacities, but their surface finishes are inherently smoother than those of large rods. Furthermore, the previous work at earth-normal and elevated gravity has shown that gravity only enters through certain dimensionless groups, but it hasn't eliminated the possibility that other groups might be important only at very low gravity. For these reasons we propose an experiment in which the relation between  $q$  and  $\Delta T$ , and other aspects of boiling, can be studied in the very low gravity environment of the space-shuttle.

The objectives of this experiment are as follows:

- 1) It should verify the existing prediction of  $q_{\max}$  for cylinders in the range  $R' > 0.1$ . (See, e.g., page 36 in [7] and the surrounding discussion.)
- 2) It should provide low gravity observations of boiling (comparable with those in Appendix A) in the ranges:  $R' < 0.01$  and  $0.01 < R' < 0.1$ . Entire curves of heat flux against temperature difference should be constructed, especially in the low  $R'$  range.

- 3) Heaters, both with higher thermal capacities, and thermal capacities comparable to those in earth-gravity experiments, should be used to avoid confusing effects of thermal capacity with those of low gravity. In particular the phenomenon of flickering should be investigated. It should be ascertained whether or not the flickering criterion developed for small wires also works at low gravity.

#### B. Approach

Geometrical considerations. The heater configuration in a low gravity boiling experiment must be a "finite" geometrical configuration. We have already seen that size and gravity are interrelated. There is thus no obvious way in which a large -- effectively infinite -- flat plate, with no characteristic dimension would reveal the special influence of reduced gravity. Indeed, an infinite plate would be hard to approximate at reduced gravity since the vapor jet spacing would be very large. The simplest and most reasonable configuration to deal with is that of a horizontal cylinder since we already have a wealth of information dealing with it. It is the configuration that we propose for study in the space shuttle.

Independent variables. The proposed experiments are designed to study systematically the influence of  $R'$  and  $g$  on boiling from horizontal cylinders. We are interested in the following three ranges of  $R'$  values:

$R' < 0.01$  (Something on the order of  $R' = 0.005$ .) This will permit observation of low-gravity boiling in the regime in which the hydrodynamic processes have vanished and there is no peak heat flux.



$0.01 < R' < 0.10$  (Something on the order of  $R' = 0.030$ .) This will facilitate observation of boiling in the transition region in which the hydrodynamic mechanisms are only partially established.

$R' > 0.10$  (Something on the order of  $R' = 0.20$ .) This will facilitate low-gravity observation of boiling in the regime in which the established hydrodynamic processes should prevail.

The experiments will be run at two reduced gravity levels:  $9.8 \times 10^{-2} \text{ m/s}^2$  and  $9.8 \times 10^{-4} \text{ m/s}^2$ . The latter is the lowest level that will be reasonably free of g-jitter effects. The former, available only in short bursts up to 45s each, is the highest level available. Together they provide two very different low-gravity levels and will allow confirmation of any scaling laws deduced from, or verified by, these tests.

Experimental Technique. The heater will be immersed in a fluid reservoir and heated electrically. We envision a set of small sealed, thermally conducting test cells, each of which contains a single cylindrical heater mounted horizontally in the minimal gravity field.

The specification of heater sizes and fluid properties which are related to  $R'$ , and the box dimensions will be discussed in subsequent sections. One reusable box will be designated for each set of test conditions; backup test cells will also be provided. A preheater will be used to raise the saturation pressure and temperature in the test cell to an appropriate level to be specified. Power will then be applied to the heater wire and increased linearly

with time until the average wire temperature reaches a preset shut-off value. Continuous heat flux, temperature, and photographic data will be obtained and subsequently used to analyze the boiling process.

If the tests are of short duration, the pressure and temperature rise in the test cell should not be excessive and no external cooling apparatus will be required. The shift in the saturation state will subsequently be shown to be small enough that it can easily be tolerated during such brief heating in a constant volume process.

It is also easy to show that the amount of evaporation is virtually negligible in such processes, thus the liquid level is practically constant. For example, in a closed container 80 percent filled with liquid water undergoing a temperature change from  $21^{\circ}\text{C}$  to  $66^{\circ}\text{C}$  only 0.04 percent of the water will evaporate. Thus the proposed technique should give nearly constant test conditions. We shall also show that the scaling parameter  $R'$  is insensitive to the cell pressure and saturation temperature.

The proposed experimental system offers many advantages, e.g.: photography can be made continuous during the run; if the temperature rises the liquid will remain saturated in the closed boxes that are used; and operator intervention is minimized. A schematic diagram of the overall experiment system is presented in Figure 1. The design and specification of the various system components, the experimental procedure, and the data reduction scheme are addressed in subsequent sections.

### C. Liquid Selection and Sizing of Heaters

The problem of selecting appropriate liquids for the experiments and the problem of setting the diameter of the test heaters are

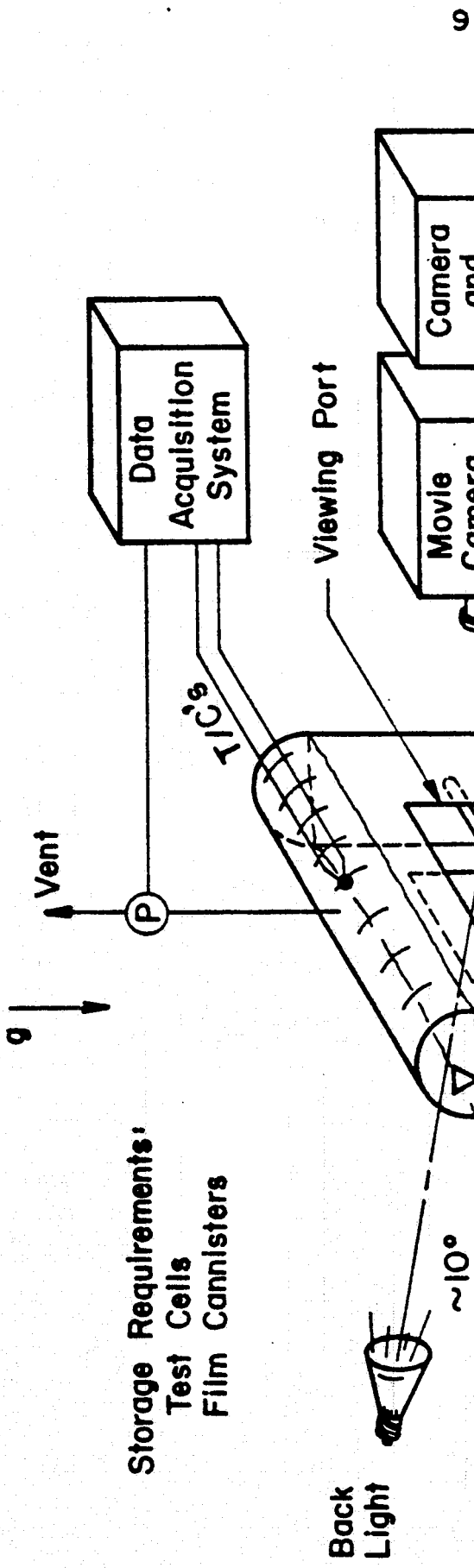


Fig. 1 Schematic Diagram of the Spacelab Pool Boiling Experiment.

interrelated through the scaling parameter,  $R'$ , and to a lesser extent through the flickering parameter,  $\Lambda$ . The fluids chosen for evaluation included those studied by Bakhru (water, benzene, methanol, acetone, and isopropanol), and two others. These were ethanol which is similar to (but less toxic than) methanol<sup>3</sup>, and Freon 113 which promises many advantages as an experimental fluid.

Physical properties. Before turning to the specification of values of  $R'$  and  $\Lambda$ , we need to identify the physical properties of the fluids. The evaluations were carried out by Bhatti and details are included in the second monthly progress report for the present work [9]. The main source of these data was a collection of data fits made earlier for NASA by Reich [10], and a DuPont report on data for Freon 113 [11]. The specific data sources are as follows:

- vapor pressure data [10], [11]
- liquid density [10], [11]
- latent heat of vaporization [10]
- vapor density [10], [11], and the ideal gas law at very low pressure.
- liquid viscosity [10], [12]
- specific heat at constant pressure, for the liquid [10], [11]
- surface tension: calculated from an earlier version of a new correlation [13]
- thermal conductivity: linear extrapolations in temperature were run through the limited data given by Reid and Sherwood [14] for the five organic liquids, through the Freon 113 data in [14], and through Bretsznajder's [15] data for water.

---

<sup>3</sup>And which, after all, can be drunk if the trip home waxes long.

- Coefficient of thermal expansion,  $\beta$ : These were obtained by differentiating Washburn's [16] liquid density formula for ethanol, Reich's densities for the remaining organic liquids [10], and densities from [11] for Freon 113.

These data are listed for four typical pressure levels in Tables 1,2,3, and 4. The numbers in these tables are generally a bit less accurate than the sources from which they were derived, since the original data were curve-fitted with equations to facilitate computerized calculations.<sup>4</sup>

Selection. As noted in the preceding section, we wish to investigate boiling in the hydrodynamic region, the non-hydrodynamic region, and the transition region, at two different low gravity conditions. Accordingly we use the data in Tables 1,2,3, and 4 to plot the heater radius that will give  $R'=0.005$ ,  $0.03$ , and  $0.2$  at  $g/g_e=10^{-2}$  and  $10^{-4}$ , as a function of pressure in Figures 2a to 2f.

These figures all reveal that the pressure can vary (as we have proposed) without influencing  $R'$  by more than a few percent in the pressure range of interest. This means that no extraordinary measures need be undertaken to keep the cell pressure at design values. This in turn will result in great simplification of the experiment.

Two factors restrict the absolute size of heaters. One is the power required by heaters of large surface area. The other is the aspect ratio, or ratio of heater length to diameter. In

---

<sup>4</sup>Generally they lie within what we could have termed "slide-rule accuracy", a scant five years ago.

Table 1.  
Properties of Saturated Liquids at a Pressure of 1 atm or 101,300 Newtons per Square Meter

Properties	Units	Water	Benzene	Acetone	Methanol	Ethanol	Isopropanol	Freon 113
Saturation Temperature (T)	$^{\circ}\text{K}$	373.1	353.2	329.3	337.9	351.5	358.6	320.8
Surface Tension ( $\sigma$ )	N/m	.05726	.02111	.01915	.01834	.01724	.01624	.01523
Density of Liquid ( $\rho_f$ )	$\text{kg/m}^3$	958.1	815.6	749.4	748.3	739.0	735.9	1510.0
Density of Vapor ( $\rho_g$ )	kg/m	0.5907	2.760	2.198	1.206	1.673	2.400	7.405
Latent heat of Vaporization ( $h_{fg}$ )	J/kg	2,257,000	399,100	549,100	1,113,000	852,400	698,800	146,800
Viscosity of Liquid ( $\mu_f$ )	N-s/m <sup>2</sup>	.000259	.000312	.000240	.000337	.000450	.000488	.000504
Specific Heat of Liquid ( $c_p$ )	J/kg- $^{\circ}\text{K}$	4103	1960	2330	2667	3277	3784	982.7
Thermal Conductivity of Liquid ( $k_f$ )	W/m $^{\circ}\text{K}$	0.6803	0.1272	0.1437	0.1942	0.1588	0.1216	.0706
Thermal Expansion Coefficient ( $\beta$ )	( $^{\circ}\text{K}$ ) <sup>-1</sup>	.000167	.000411	.000464	.000394	.000892	.000320	.000508
$\sqrt{\sigma/g_e (\rho_f - \rho_g)}$	m	.002467	.001627	.001617	.001582	.001544	.001502	.001016

Table 2.  
Properties of Saturated Liquids at a Pressure of 0.6684 atm or 67,730 Newtons per Square Meter

Properties	Units	Water	Benzene	Acetone	Methanol	Ethanol	Isopropanol	Freon 113
Saturation Temperature (T)	$^{\circ}\text{K}$	362.2	340.7	318.0	327.9	341.6	348.8	309.1
Surface Tension ( $\sigma$ )	N/m	.05929	.02240	.02031	.01918	.01804	.01699	.01630
Density of Liquid ( $\rho_f$ )	$\text{kg}/\text{m}^3$	965.7	828.9	762.2	751.7	747.3	743.4	1539
Density of Vapor ( $\rho_g$ )	$\text{kg}/\text{m}^3$	0.4042	1.912	1.494	0.8260	1.140	1.643	5.068
Latent heat of Vaporization ( $h_{fg}$ )	J/kg	2,284,000	407,900	566,900	1,133,000	866,800	734,700	150,500
Viscosity of Liquid ( $\mu_f$ )	$\text{N}\cdot\text{s}/\text{m}^2$	.0003061	.0003599	.0002671	.0003824	.0005310	.0006052	.0005762
Specific Heat of Liquid ( $c_p$ )	$\text{J}/\text{kg}\cdot^{\circ}\text{K}$	4099	1908	2287	2632	3114	3632	969.2
Thermal Conductivity of Liquid ( $k_f$ )	$\text{W}/\text{m}\cdot^{\circ}\text{K}$	0.6748	0.1316	0.1492	0.1974	0.1615	0.1293	.07285
Thermal Expansion Coefficient ( $\beta$ )	$(^{\circ}\text{K})^{-1}$	.0001665	.0004042	.0004564	.0003887	.0009373	.0003171	.0004833
$\sqrt{\sigma/g_e (\rho_f - \rho_g)}$	m	.002503	.001662	.001650	.001608	.001570	.001528	.001041

Table 3.  
 Properties of Saturated Liquids at a Pressure of 0.3342 atm or 33,860 Newtons per Square Meter

Properties	Units	Water	Benzene	Acetone	Methanol	Ethanol	Isopropanol	Freon 113
Saturation Temperature (T)	$^{\circ}\text{K}$	345.1	321.4	300.5	312.3	326.1	333.8	291.5
Surface Tension ( $\sigma$ )	N/m	.06243	.02435	.02205	.02047	.01925	.01809	.01791
Density of Liquid ( $\rho_f$ )	$\text{kg/m}^3$	976.9	849.4	782	772.6	760.4	754.9	1580
Density of Vapor ( $\rho_g$ )	kg/m	0.2061	0.9984	0.7978	0.4251	0.5896	0.8746	2.659
Latent heat of Vaporization ( $h_{fg}$ )	J/kg	2,326,000	421,300	594,400	1,165,000	889,600	789,500	155,600
Viscosity of Liquid ( $\mu_f$ )	N-s/m <sup>2</sup>	.0004001	.0004525	.0003179	.0004593	.0007290	.0008488	.0007198
Specific Heat of Liquid ( $c_p$ )	J/kg- $^{\circ}\text{K}$	4093	1827	2221	2576	2857	3400	949.6
Thermal Conductivity of Liquid ( $k_f$ )	W/m $^{\circ}\text{K}$	0.6643	0.1383	0.1577	0.2025	0.1658	0.1341	7.648
Thermal Expansion Coefficient ( $\beta$ )	( $^{\circ}\text{K}$ ) <sup>-1</sup>	.0001692	.0003943	.0004449	.0003811	.0009929	.0003123	.0004478
$\sqrt{\sigma/g_e (\rho_f - \rho_g)}$	m	.002553	.001711	.001697	.001644	.001607	.001564	.001076



Table 4.  
Properties of Saturated Liquids at a Pressure of 0.0668 atm or 6,773 Newtons per Square Meter

Properties	Units	Water	Benzene	Acetone	Methanol	Ethanol	Isopropanol	Freon 113
Saturation Temperature (T)	$^{\circ}\text{K}$	311.6	285.3	267.4	281.8	295.7	306.2	258.2
Surface Tension ( $\sigma$ )	N/m	.06842	.02791	.02522	.02284	.02149	.02000	.02083
Density of Liquid ( $\rho_f$ )	$\text{kg/m}^3$	993	887.7	819.3	801.5	786.1	776.2	1653
Density of Vapor ( $\rho_g$ )	kg/m	.04924	0.2420	0.1769	.09342	0.1267	0.2229	0.5942
Latent heat of Vaporization ( $h_{fg}$ )	J/kg	2,410,000	446,600	646,300	1,226,000	934,100	890,700	164,200
Viscosity of Liquid ( $\mu_f$ )	N-s/m <sup>2</sup>	.0007226	.0007366	.0004031	.0007090	.001716	.001618	.001201
Specific Heat of Liquid ( $c_p$ )	J/kg- $^{\circ}\text{K}$	4080	1675	2097	2467	2354	2971	892.9
Thermal Conductivity of Liquid ( $k_f$ )	W/m $^{\circ}\text{K}$	0.6258	0.1509	0.1738	0.2122	0.1742	0.1430	.08339
Thermal Expansion Coefficient ( $\beta$ )	( $^{\circ}\text{K}$ ) <sup>-1</sup>	.0001620	.0003769	.0004246	.0003673	.001049	.0003038	.0003871
$\sqrt{\sigma/g_e (\rho_f - \rho_g)}$	m	.002651	.001791	.001772	.001705	.001670	.001621	.001134

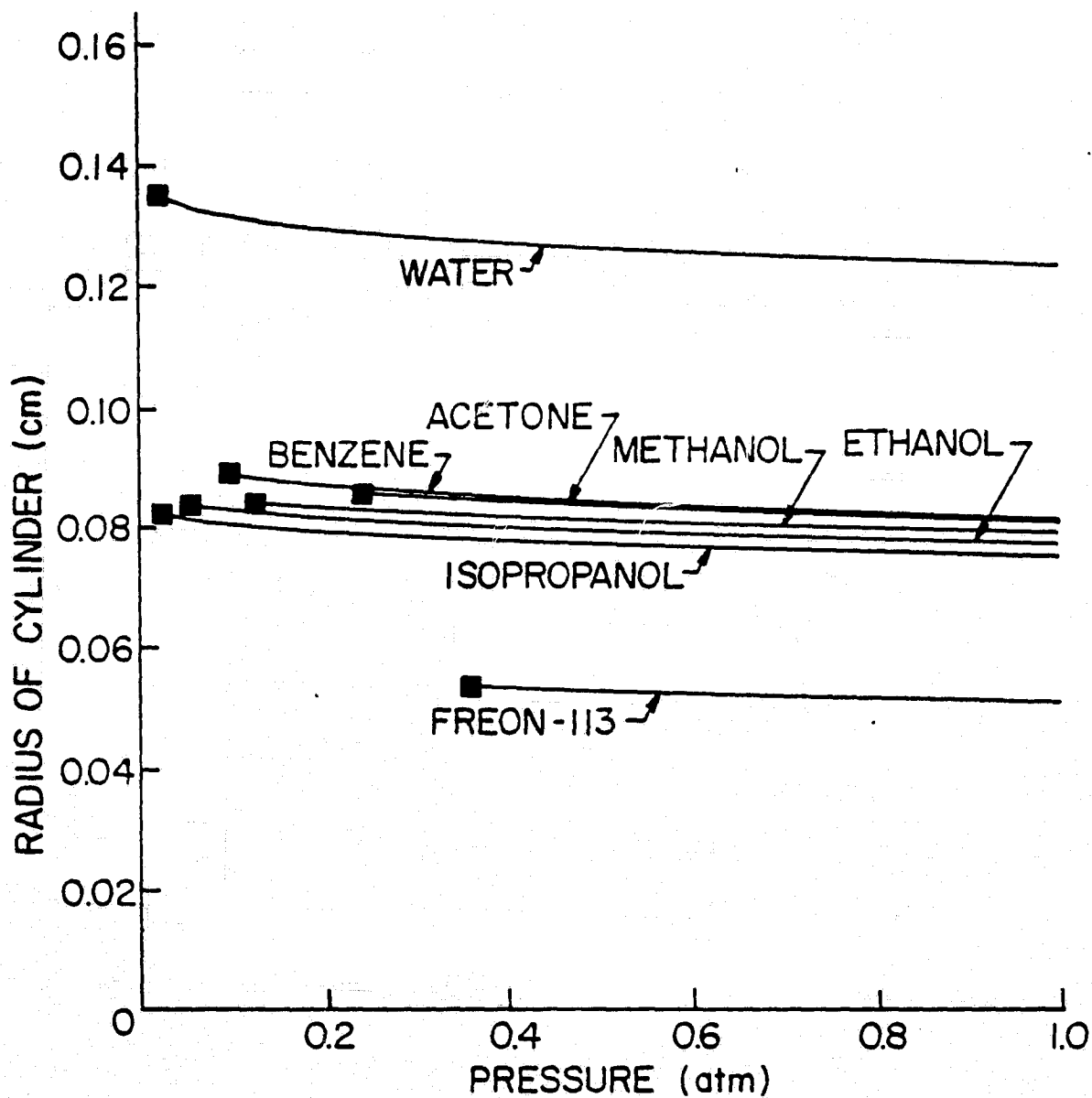


Fig. 2a Variation of heater radius with pressure for  $R' = 0.005$   
and  $\frac{g}{g_e} = 10^{-4}$

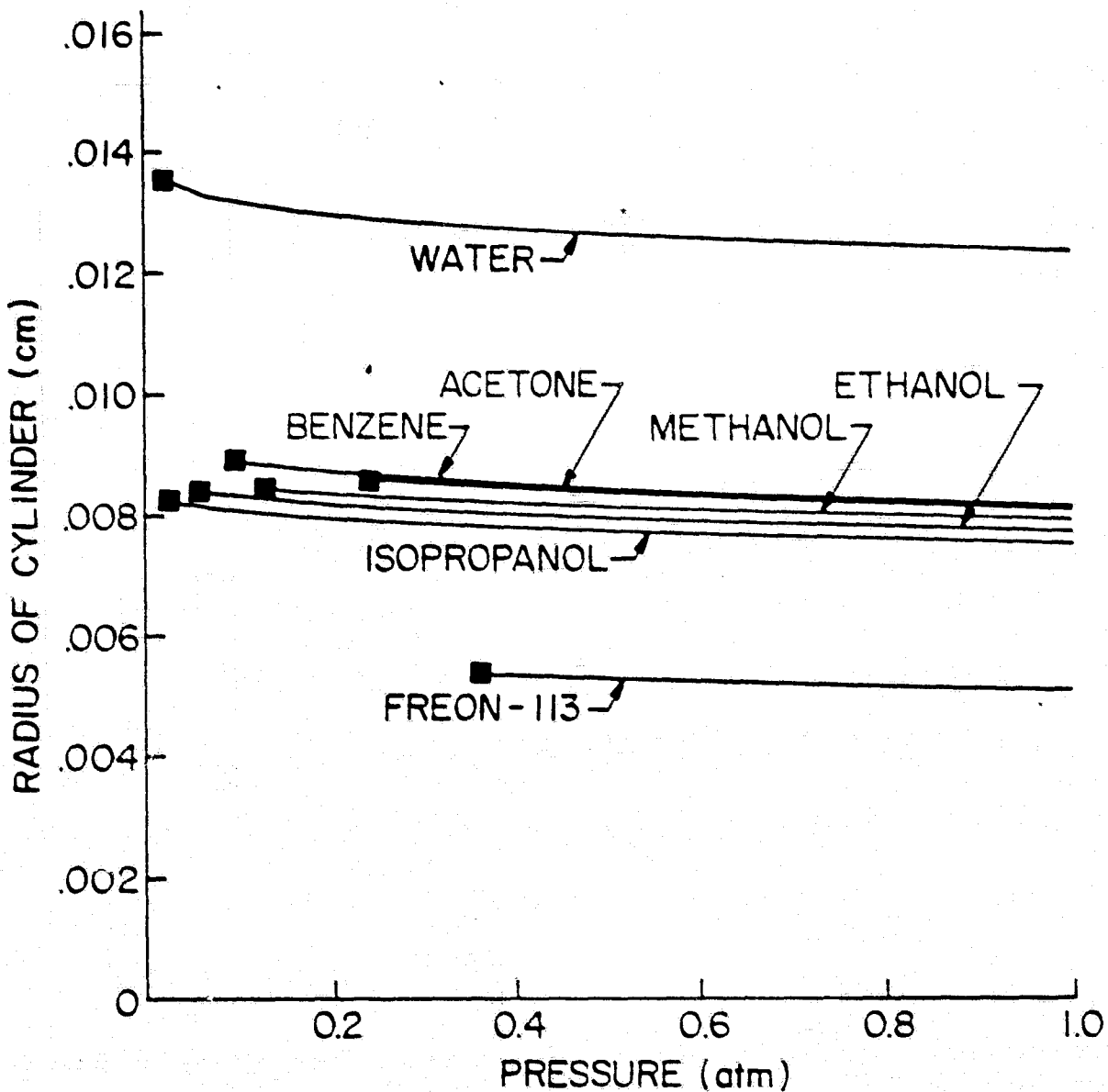


Fig. 2b Variation of heater radius with pressure for  $R' = 0.005$   
and  $\frac{g}{g_e} = 10^{-2}$

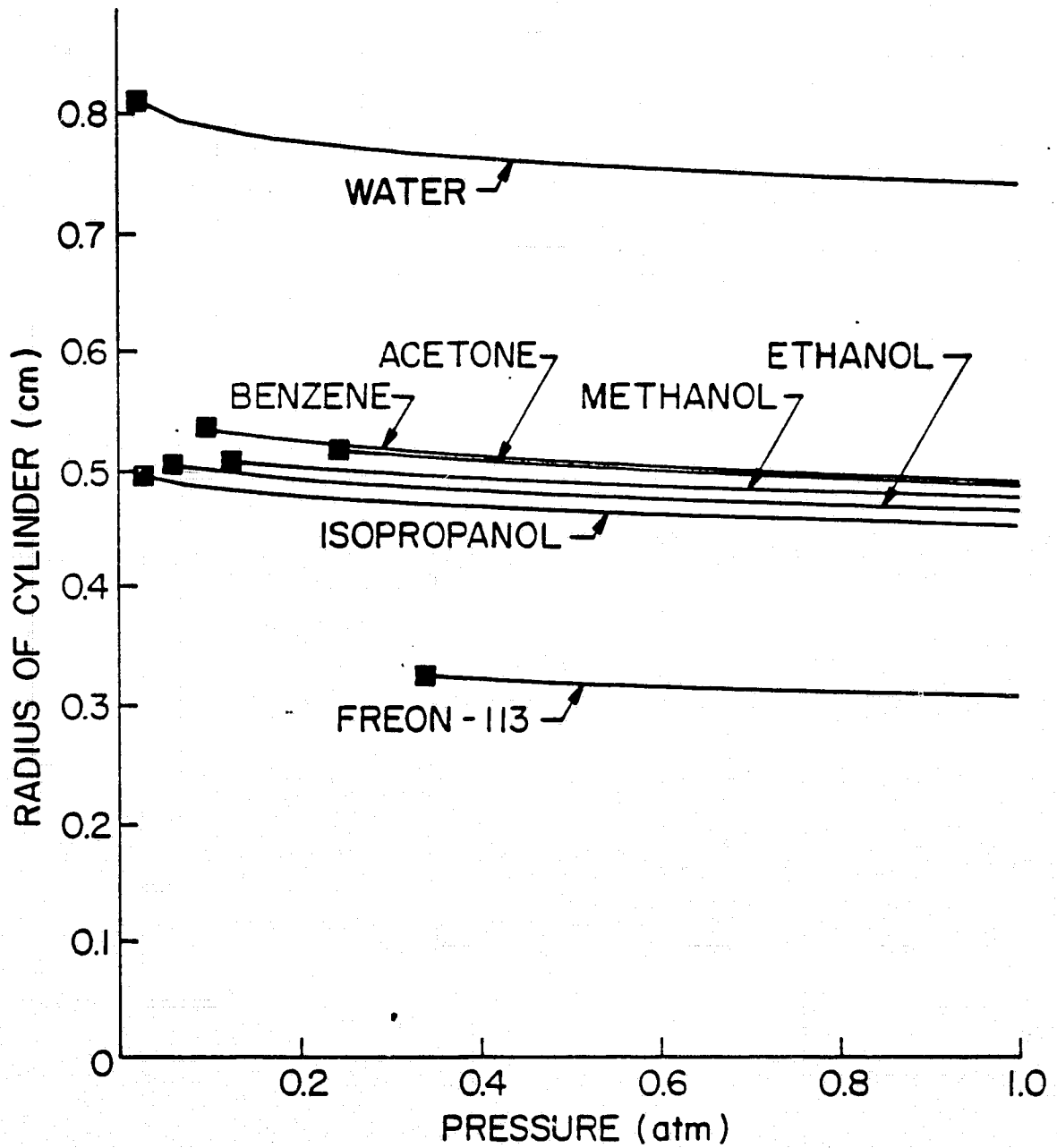


Fig. 2c Variation of heater radius with pressure for  $R' = 0.03$   
and  $\frac{g}{g_e} = 10^{-4}$ .

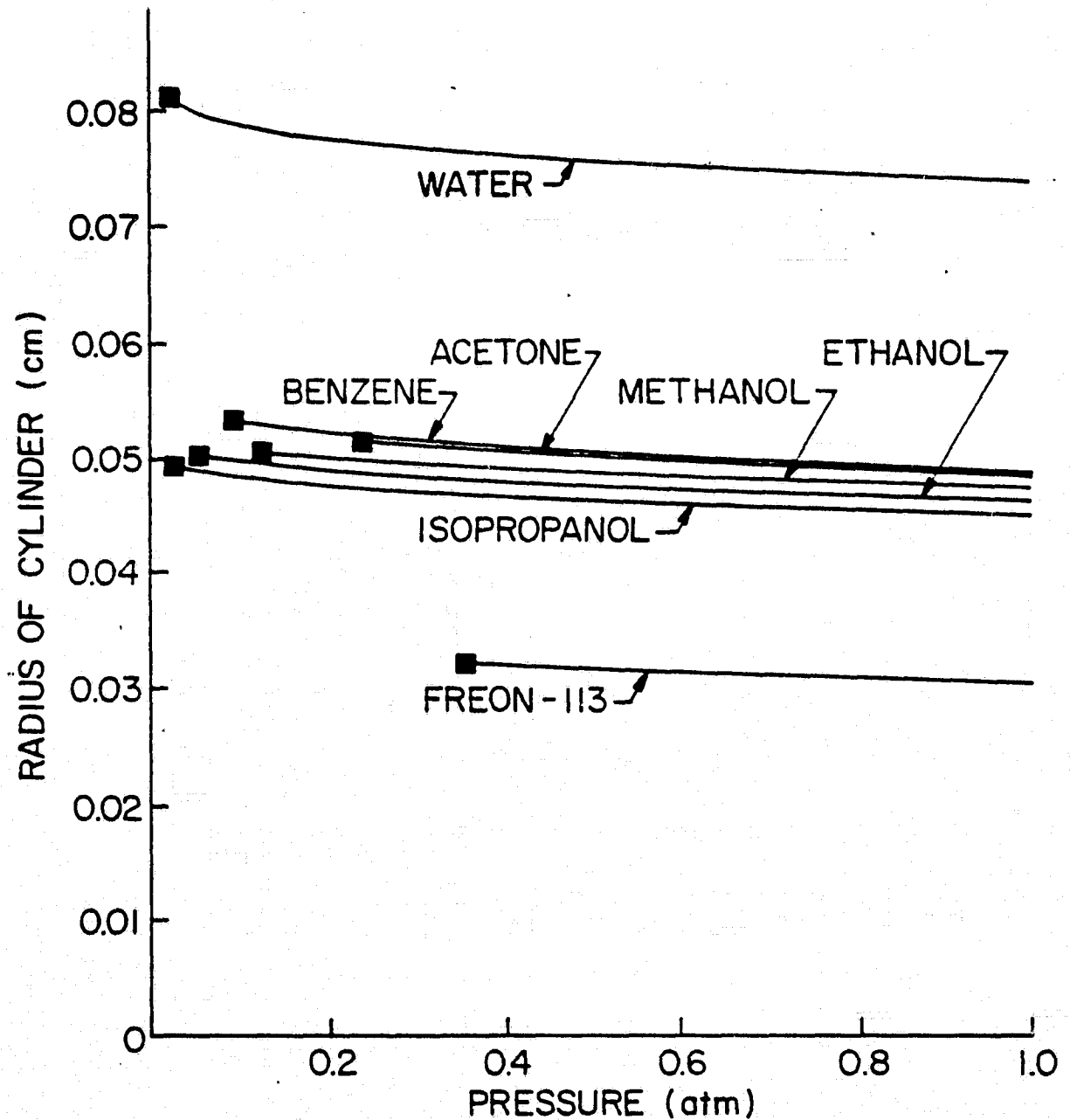


Fig. 2d Variation of heater radius with pressure for  $R' = 0.03$   
and  $\frac{g}{g_e} = 10^{-2}$

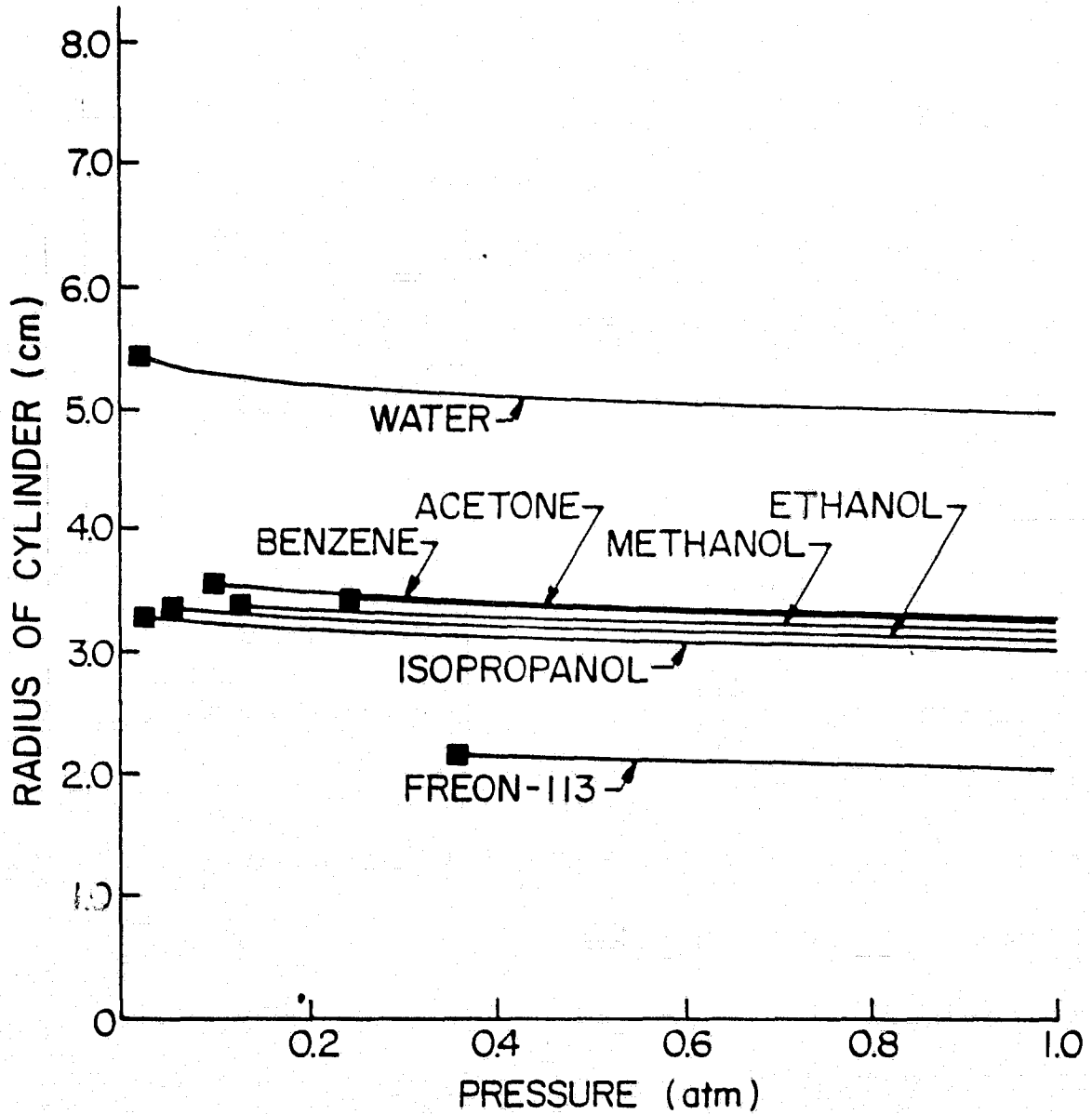


Fig. 2e Variation of heater radius with pressure for  $R' = 0.2$  and  $\frac{g}{g_e} = 10^{-4}$

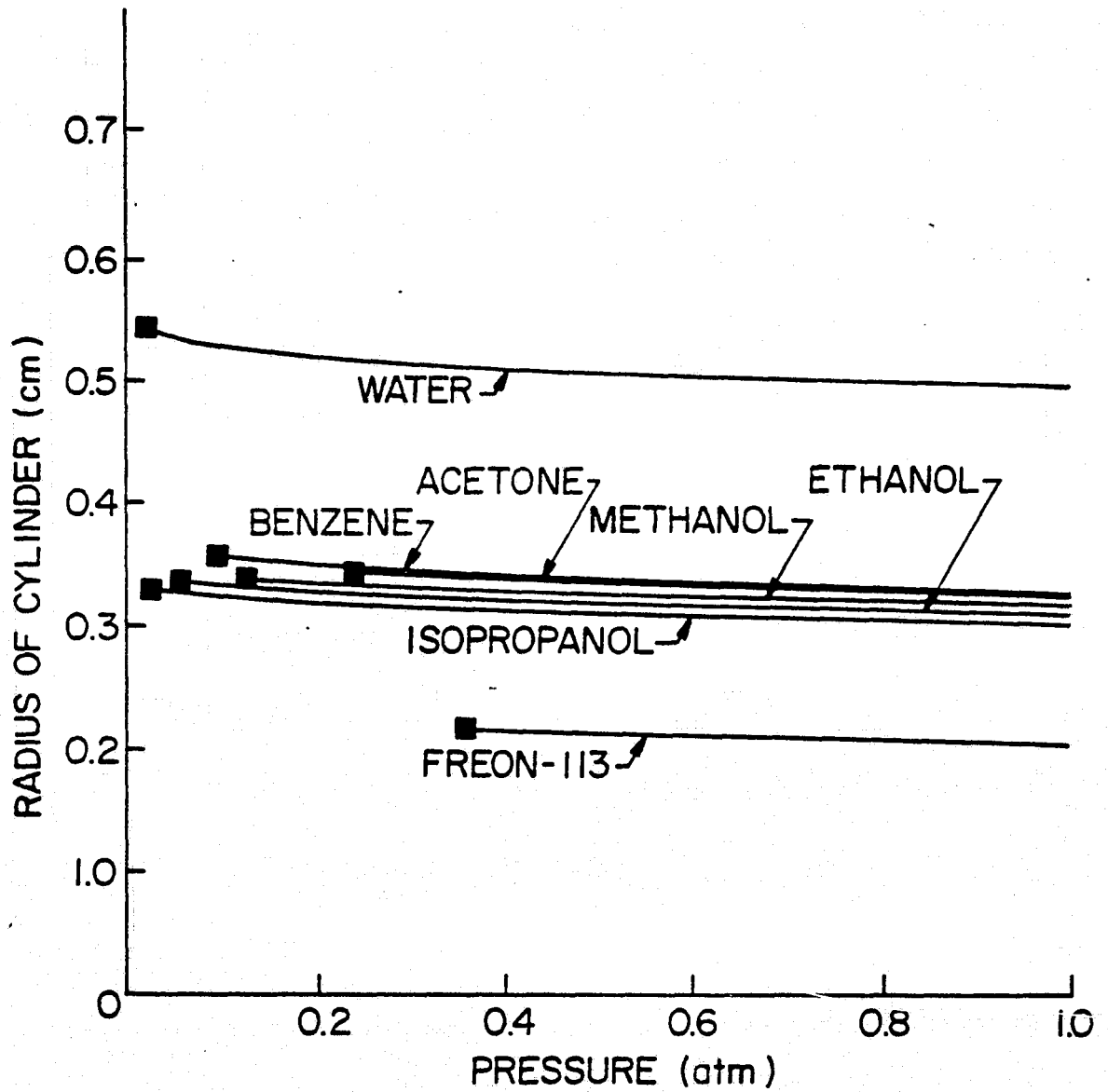


Fig. 2f Variation of heater radius with pressure for  $R' = 0.2$   
and  $\frac{g}{g_e} = 10^{-2}$ .

Bakhru's experiments this ratio was on the order of  $10^3$  so that end effects were inconsequential. We should like to keep this ratio as large as possible.

Figure 2e shows clearly that no experiments should be attempted at the lower gravity level with  $R'=0.2$  since the heaters would be too large.

There are basically three reasonable choices of fluids: water, Freon 113, and one from among the remaining organic substances. We shall eliminate all but one of the organic liquids:

benzene: Because it is too toxic and highly flammable.

ethanol: Because it was not among Bakhru's liquids, while the rest of this group was.

acetone and isopropanol: Since Bakhru reported only one run with each of them.

Methanol remains. Bakhru provided data for six values of  $R'$  in methanol. It is not toxic in modest dilution with air and it is less incendiary than acetone or benzene. Thus we specify water, Freon 113, and methanol for use in the experiment.

The water-filled container will be used to observe fairly small platinum cylinders at low pressure and  $R'=0.005$  or less. The largest of these can also be run at  $R'=0.03$  under  $10^{-2} g_{\text{earth}}$  conditions. Sizes in the water capsule will include:



Condition	2xR, cm	g/g <sub>e</sub>	R'	press, atm.	T <sup>o</sup> C
1	0.1524	10 <sup>-4</sup>	0.003	0.17	57
2	0.1524	10 <sup>-2</sup>	0.03	0.17	57
3	0.0254	10 <sup>-4</sup>	0.0005	0.17	57
4	0.0254	10 <sup>-2</sup>	0.005	0.17	57

The methanol filled container will be used to observe both large and small heaters under all three conditions of R'.

Condition	2xR, cm	g/g <sub>e</sub>	R'	press, atm.	T <sup>o</sup> C
5	0.64	10 <sup>-2</sup>	0.2	0.33	39
6	0.64	10 <sup>-4</sup>	0.02	0.33	39
7	0.17	10 <sup>-4</sup>	0.005	0.33	39
8	0.10	10 <sup>-2</sup>	0.03	0.33	39

The Freon-filled container will also be used to observe the range of R' values.

Condition	2xR, cm	g/g <sub>e</sub>	R'	press, atm.	T <sup>o</sup> C
9	0.061	10 <sup>-4</sup>	0.003	0.67	36
10	0.061	10 <sup>-2</sup>	0.03	0.67	36
11	0.61	10 <sup>-4</sup>	0.03	0.67	36
12	0.61	10 <sup>-2</sup>	0.3	0.67	36

Thus we propose twelve basic runs. Six are to be at elevated gravity and six are at the lower gravity level. The sizes above are not precise. They can be altered slightly with unimportant proportional alterations in  $R'$ . Thus we can standardize on five heater sizes. The lengths of the wires will be specified as 19 cm for the two largest (0.61 and 0.64 cm dia.) wires and 5.1 cm for the remaining ones. This will give a minimum length to diameter ratio of 30 which should be sufficient.

The Flickering Phenomenon. The flickering parameter,  $\Lambda$ , involves the heat transfer coefficient,  $h$ , at the inception of boiling. This is a natural convection value, and to calculate it we use the expression recommended by Bakhru on the basis of Herman's equation, subjected to Langmuir's correction:

$$h = \frac{2k_f}{D \ln (1 + 5/Ra_D^{1/4})} \quad (4)$$

where  $k_f$  is the thermal conductivity to the liquid,  $D$  is the diameter of the cylinder and  $Ra_D$  is the Rayleigh number based on diameter. Thus equation (3) can be expressed as:

$$\Lambda \Delta T = \frac{4\sigma_{fg} T_{sat}}{Dh_{fg} \ln \left[ 1 + 5 \left( \frac{\mu k}{g\beta \Delta T D^3 \rho_f^2 c_{P_f}} \right)^{1/4} \right]} \quad (5)$$

The problem with the use of equation (5) is that we do not know the inception temperature,  $\Delta T$ , and any attempt to predict it will be chancy. Bakhru's values, obtained for very small wires, might serve as an upper bound. This would appear to be reasonable because on Bakhru's small wires the first nucleation corresponds with a site

density,  $n$ , of about 10 active nucleation sites per  $\text{cm}^2$ . It could not begin at a lesser value because, on his small wires,  $n > 10/\text{cm}^2$  when the first bubble nucleated. The site density at which sites begin to reinforce one another so as to enhance heat transfer is far less than this -- about  $0.3 \text{ sites}/\text{cm}^2$  [17]. Thus, if a wire is larger, we can surely expect a far lower value of  $n$ , and with it a lower  $\Delta T$ , at inception.

Bakhr'u's inception values of  $\Delta T$  were about  $40^\circ\text{C}$  for water and  $44^\circ\text{C}$  for methanol. For Freon 113,  $\Delta T$  could be either larger or smaller. However, the tendency of  $\Delta T$  for organic liquids is to exceed the value for water. Since Freon 113 is "on the other side of the organics from water" (lower latent heat and vapor pressure, for example) we shall conservatively guess that  $\Delta T$  is about  $70^\circ\text{C}$  in this case.

These extremely rough estimates of  $\Delta T$  are used to estimate the R.H.S. of equation (5) since it is very weakly dependent on  $\Delta T$ . The resulting values of  $\Lambda \Delta T$  are plotted as a function of pressure, heater size, and liquid in Figure 3.

With reference to Figure 3, and recalling that Bakhr'u showed only that:

flickering definitely occurred when  $\Lambda < 0.02$ ,

flickering did not occur when  $\Lambda > 0.17$ , and

the flickering situation was unknown in between,

we can anticipate what will happen in the proposed tests:

- Freon on the smallest wire would definitely not flicker, only if  $\Delta T$  were as small as  $1^\circ\text{C}$ . Since we expect  $\Delta T \gg 1^\circ\text{C}$ , anything can happen. (It probably will flicker.)

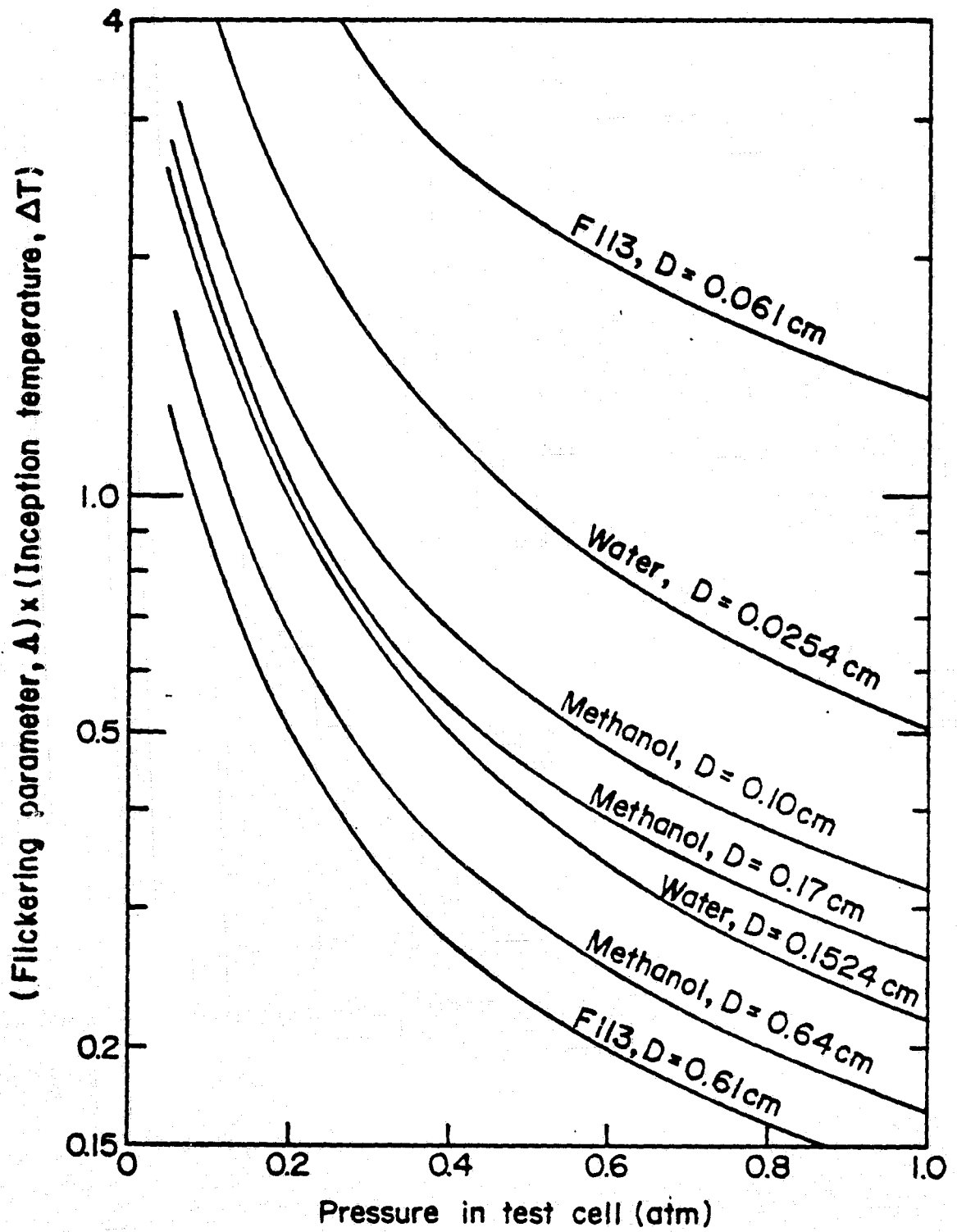


Fig. 3 Dependence of the flickering parameter on system variables.

- The larger wire that is used in water probably will flicker.
- Methanol will most likely fall in the unknown region, except for the largest heater which can function in the established flickering region if  $\Delta T$  is less than  $20^{\circ}\text{C}$ .
- The smaller wire that is used in water will probably be in the indeterminate region.
- Freon on the large wire should definitely flicker.

Thus, the proposed experiments promise to test Bakhru's flickering correlation over the full range of possibilities and to further delineate that correlation.

Thermal Capacity. Thermal capacity poses a problem which can easily be sidestepped. Appendix A (see pages A-10 and A-11) shows that the flickering phenomenon depends upon a Péclet number and a Biot number. The Biot number would remain unimportant in the phenomenon unless the cylinder radius were increased to more than 1 cm, in the case of a platinum wire. The Péclet number is a dimensionless velocity of the vapor patch front and the analysis suggests that to maintain similar behavior, the physical velocity must slow as  $1/\sqrt{R}$ . These difficulties will be overcome, and similarity with the small wire behavior will be maintained, by using a thin layer of resistance heater material plated onto an insulating cylinder.

#### D. Heat Flux Predictions

In the present section we estimate the cylinder heat fluxes that will enable us to observe the complete boiling process for each of the twelve test conditions identified in the preceding section. This information will allow us to complete the heater design and to specify the heater power requirements. We may also

assess the need for external cooling to maintain the various test cells at the desired saturation conditions. The heat flux data are presented in a series of curves (Figures 4a-f) which display cylinder heat flux as a function of the temperature difference between the heater surface ( $T_{\text{wall}}$ ) and the bulk fluid saturation temperature ( $T_{\text{sat}}$ ) for each of the twelve test environments.

The curves represent the initial (natural convection) and final (film boiling) heat fluxes for increasing heater temperatures. The natural convection heat flux for small wires was calculated using the heat transfer coefficient from equation (4). The film boiling heat transfer coefficient was obtained from equation (19) in Appendix A. Fluid properties were evaluated at  $(T_{\text{wall}} + T_{\text{sat}})/2$ .

The curves do not predict where the transition from natural convection to film boiling will occur, but indicate for design purposes the expected range of temperatures and power requirements. The actual transition point will be learned from the spacelab experiments. Since film boiling should be well-established below  $\Delta T = 500^{\circ}\text{C}$ , we will designate this temperature difference as a reference point for terminating each test run and for determining the maximum heat load requirements. It should be noted that the heater power requirements do not exceed 120 watts in any case.

#### E. Mechanical Design

The test heaters. The test heaters will be electrical resistance heaters supplied by a low voltage battery that is independent of the higher voltage cabin power supply. The temperature of all heaters will be obtained by thermocouples which give a sequence of local measurements along the inside of a thin tubular resistance heater.

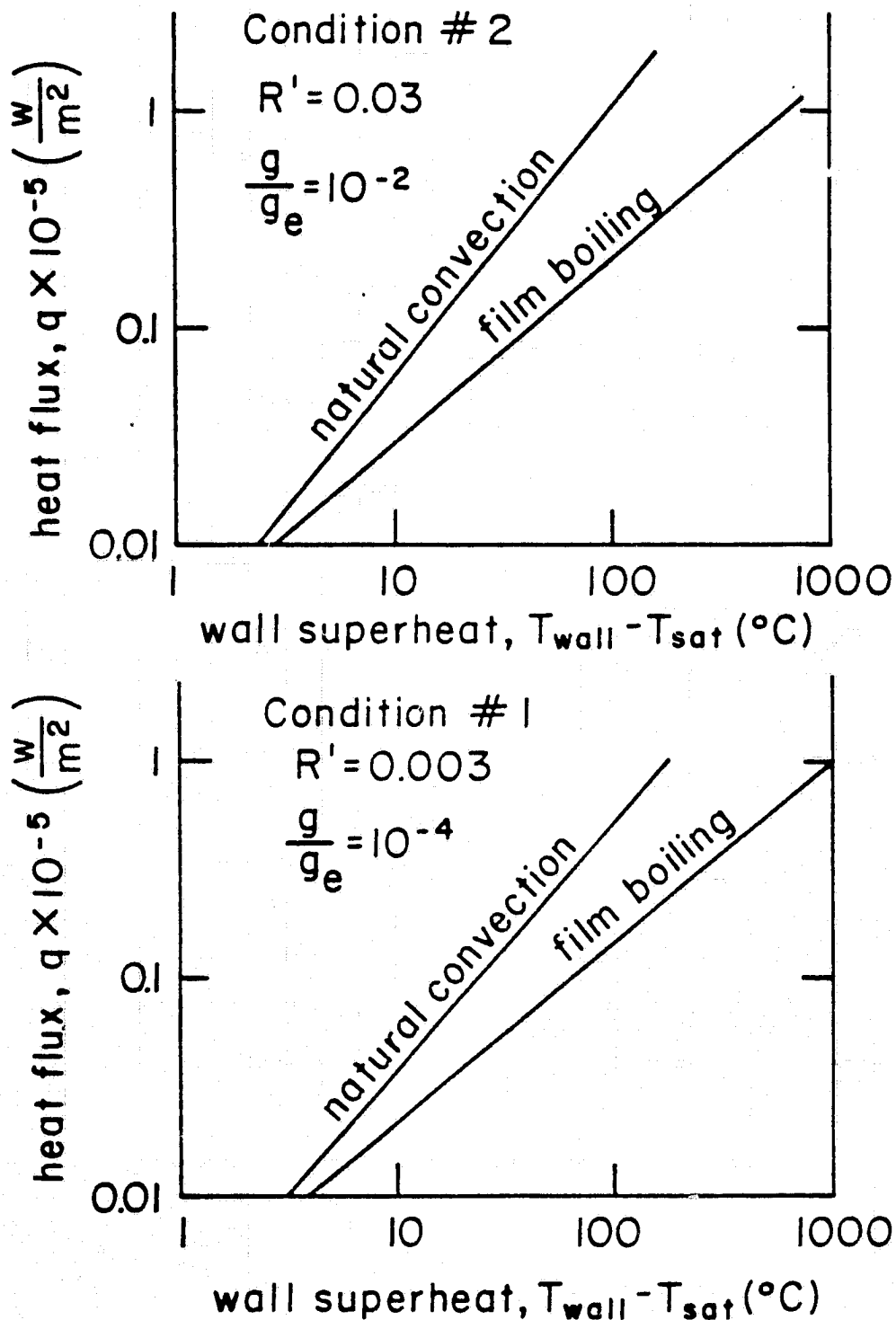


Fig. 4a Predicted heat removal from a 0.1524 cm cylindrical platinum heater in water:  $p_{sat} = 0.17 \text{ atm}$ ,  $T_{sat} = 57^\circ C$

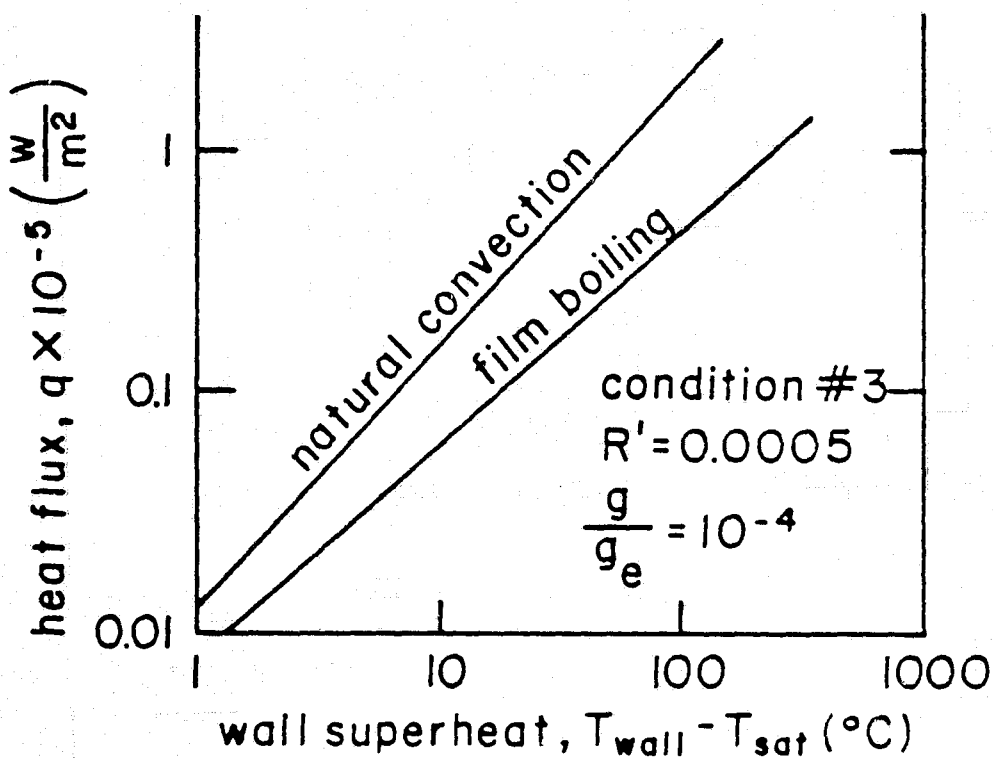
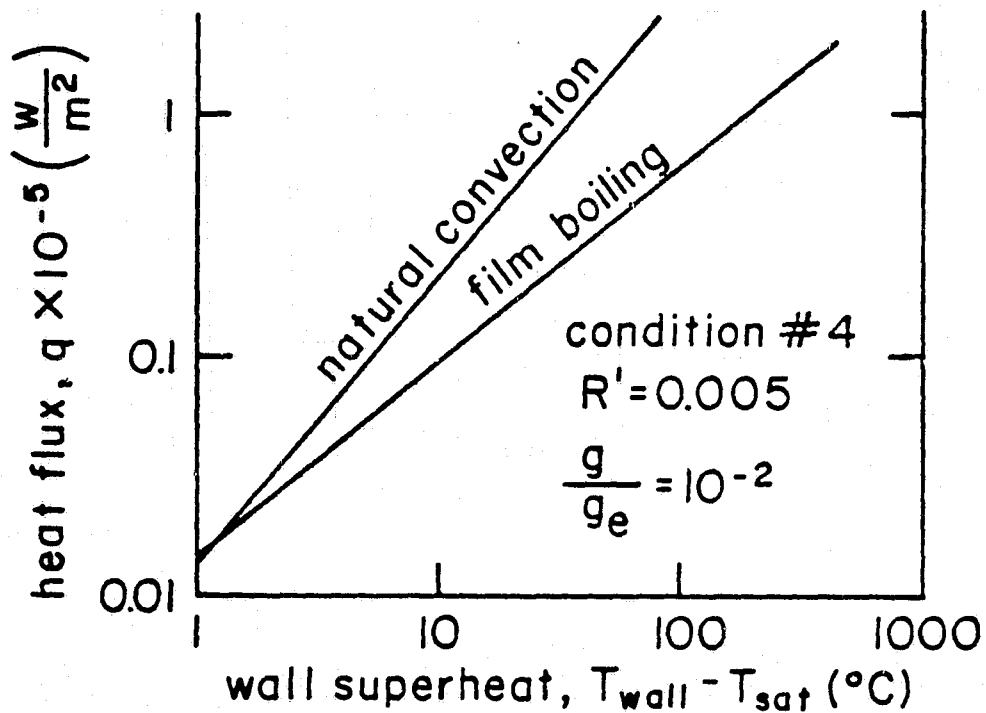


Fig. 4b Predicted heat removal from a 0.0254 cm cylindrical platinum heater in water:  $p_{\text{sat}} = 0.17 \text{ atm}$ ,  $T_{\text{sat}} = 57^\circ\text{C}$



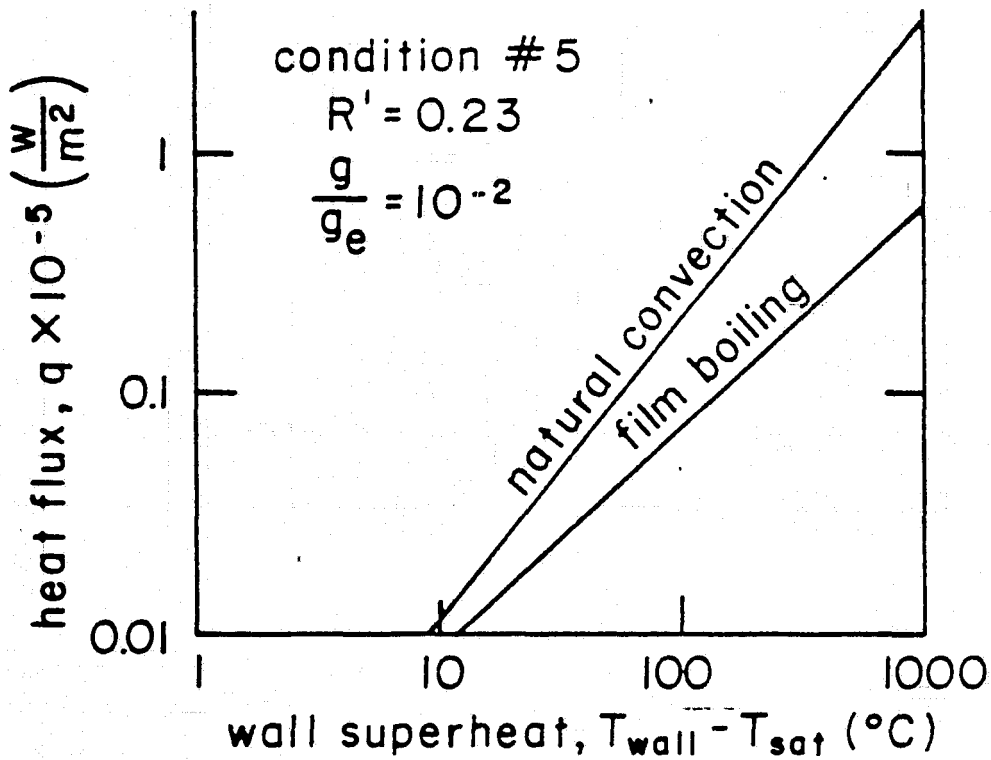
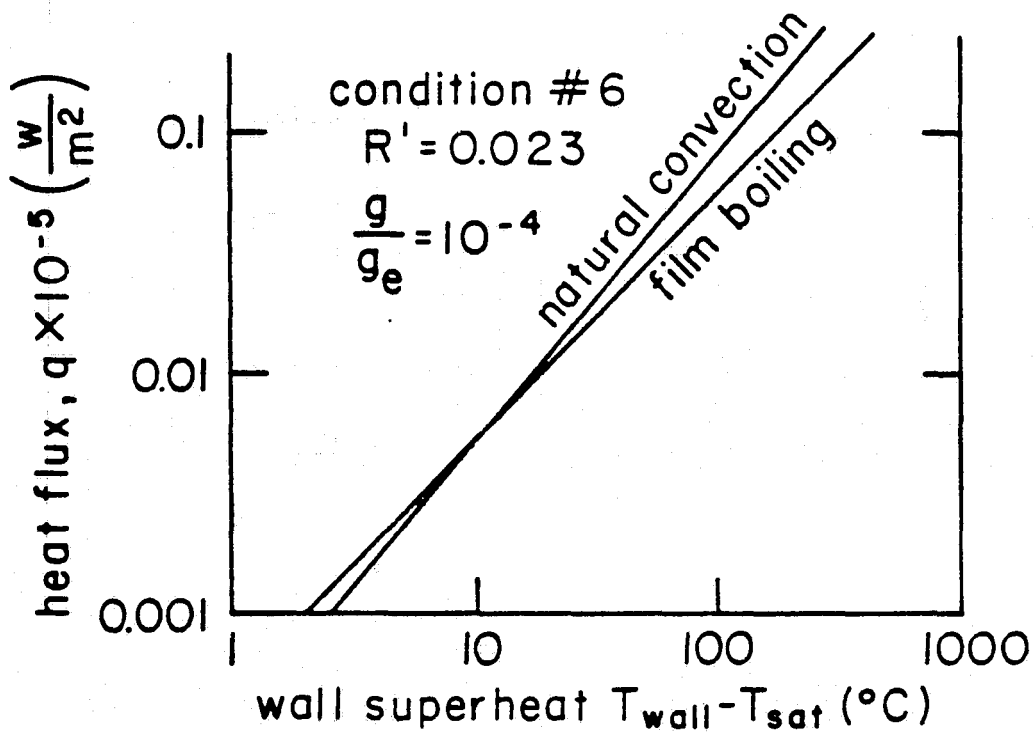


Fig. 4c Predicted heat removal from a 0.635 cm cylindrical platinum heater in methanol:  
 $p_{sat} = 0.33 \text{ atm}$ ,  $T_{sat} = 39^\circ\text{C}$

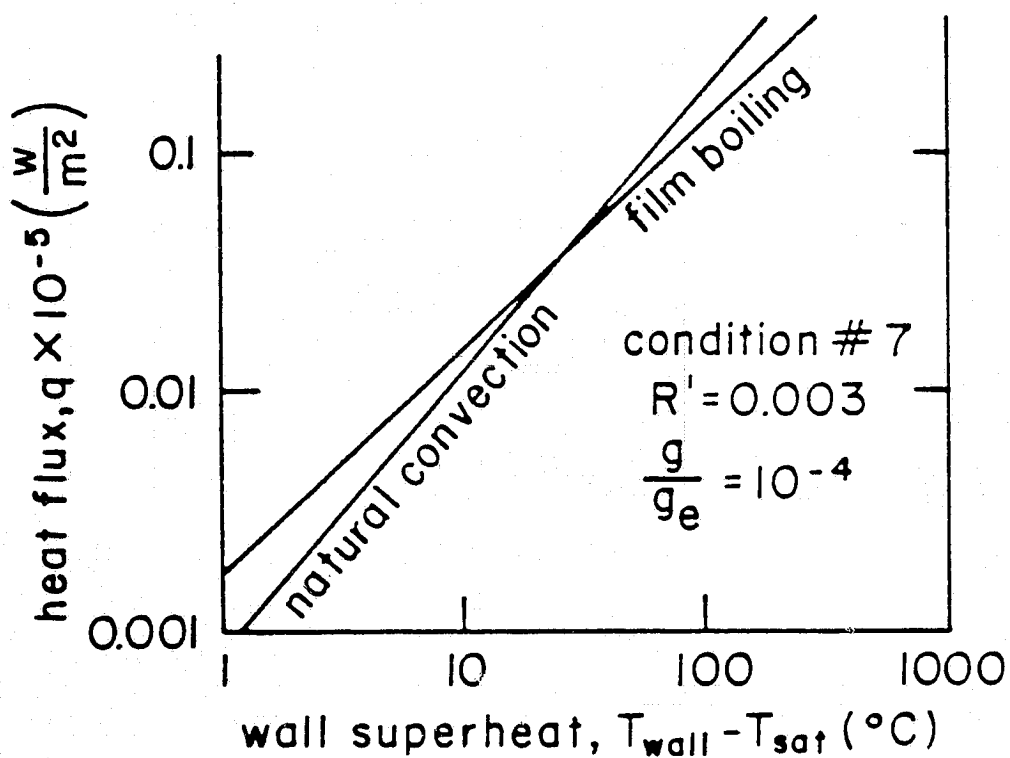
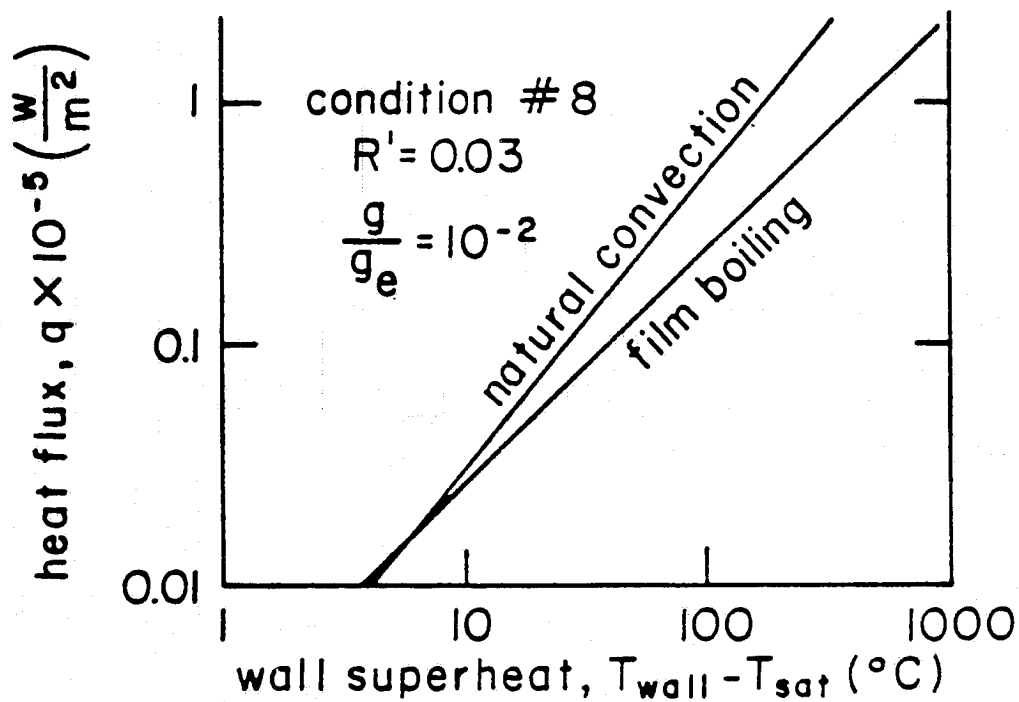


Fig. 4d Predicted heat removal from a 0.17 cm cylindrical platinum heater in methanol:  $p_{sat} = 0.33 \text{ atm}$ ,  $T_{sat} = 39^\circ\text{C}$

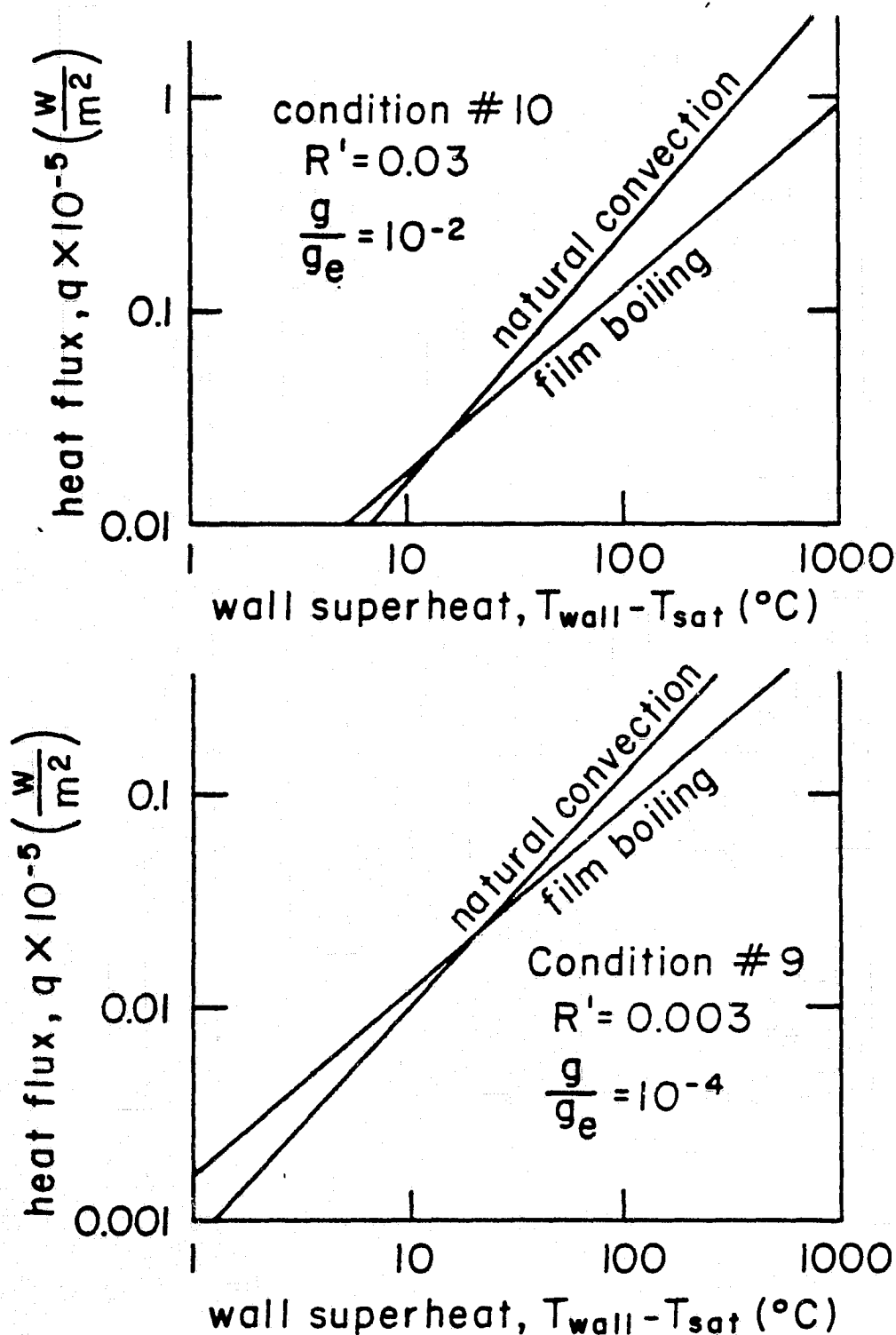


Fig. 4e Predicted heat removal from a 0.061cm cylindrical platinum heater in Freon 113:  $P_{sat} = 0.67 \text{ atm}$ ,  $T_{sat} = 36^\circ C$

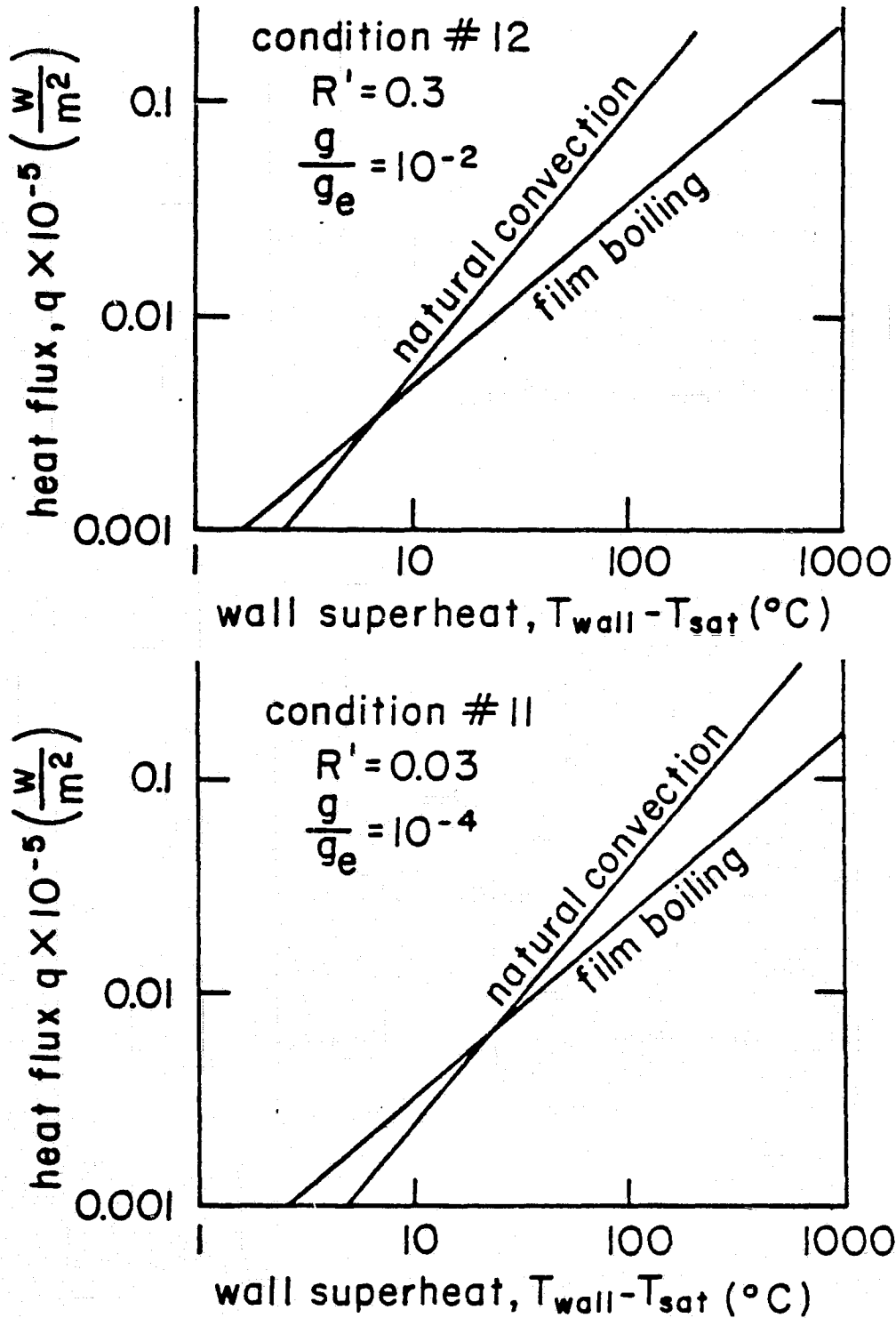
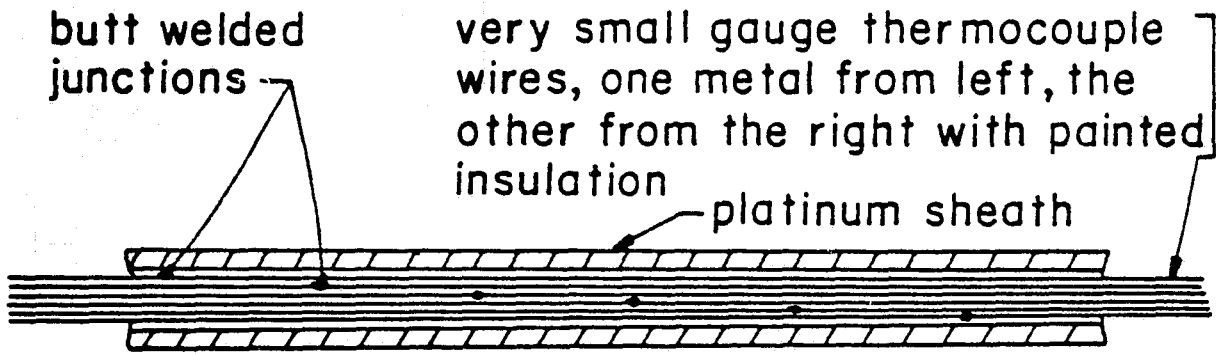


Fig. 4f Predicted heat removal from a 0.61cm cylindrical platinum heater in Freon 113:  $p_{sat} = 0.67 \text{ atm}$ ,  $T_{sat} = 36^\circ \text{ C}$

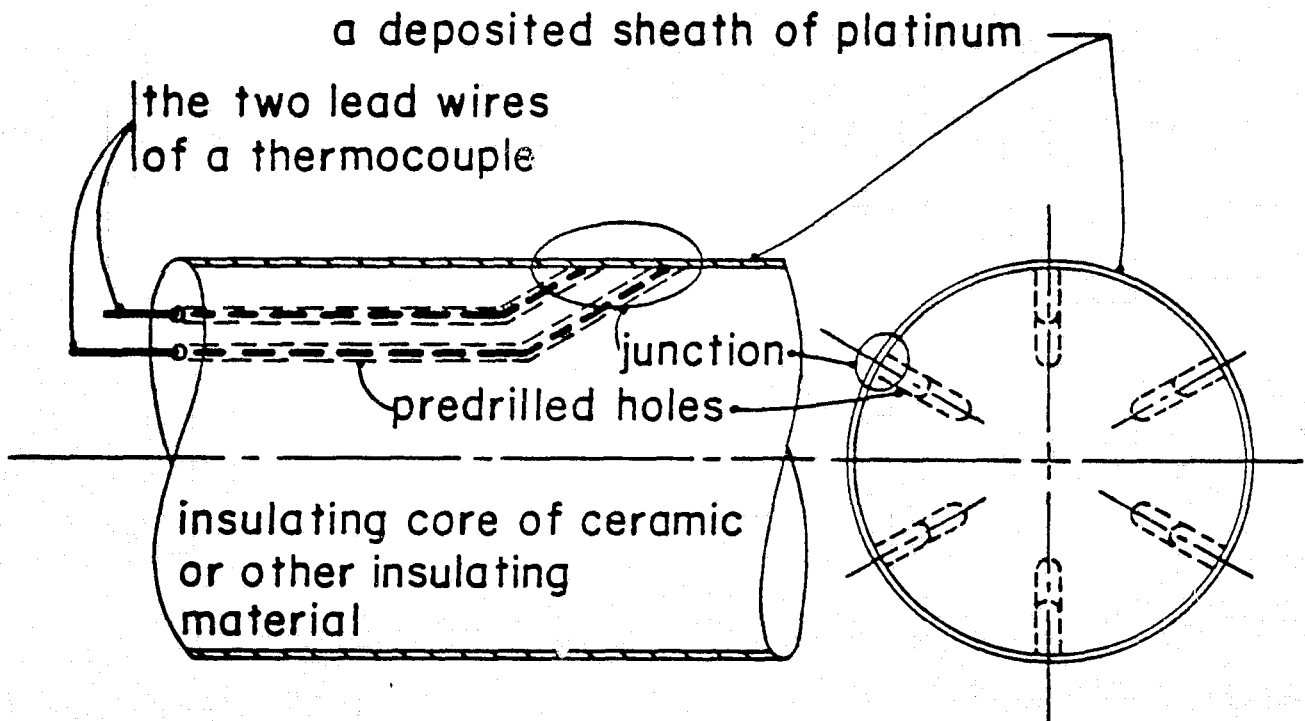
These heaters will be of two basic types: 1) thin small-bore tubing for all diameters 0.17 cm or less, and 2) heating cylinders which have been electroplated or sputtered or otherwise deposited onto dielectric elements in which the thermocouples have been embedded, for the large diameter elements. A standard wall thickness of .0051 cm is chosen for the tubular heaters, and a platinum layer of .00254 cm is to be electroplated on the surface of the larger ceramic core heaters. The two arrangements are depicted at the top and bottom, respectively, of Figure 5.

In each case we propose at least six thermocouples which will be led out of the box through the rod, as shown. The thermocouples should probably be chromel-alumel, although that decision could be influenced by the plating process in the case of the larger rods.

The configuration of the electrical connection to the rod can best be arranged as follows: A tapered copper sheath should be affixed to each end as shown in Figure 6. Such a sheath can very effectively be made by the electro-deposition of copper onto the platinum. Whether or not the entire sheath is deposited, or a larger diameter copper element is soldered onto a thin sheath which has been electro-deposited, does not matter. The length of the sheath should be such as to allow a clear run of 5.1 cm of the small rods between the sheaths, and 19.0 cm of the large rods. They should extend far enough outside of the box to accommodate the necessary electrical connections. The sheath design shown here will serve the purposes of: minimizing end effects, carrying current to the rod, and eliminating voltage drop between the test length of the rod and the outside of the box. Since we have now specified the heater dimensions, we may examine the heat removal curves (Figures 4a-f) to resolve the power requirements.



### The Small Rod Configuration



### Large Rod Configuration

Fig. 5 The configuration of heater rods with six thermocouples in each one.

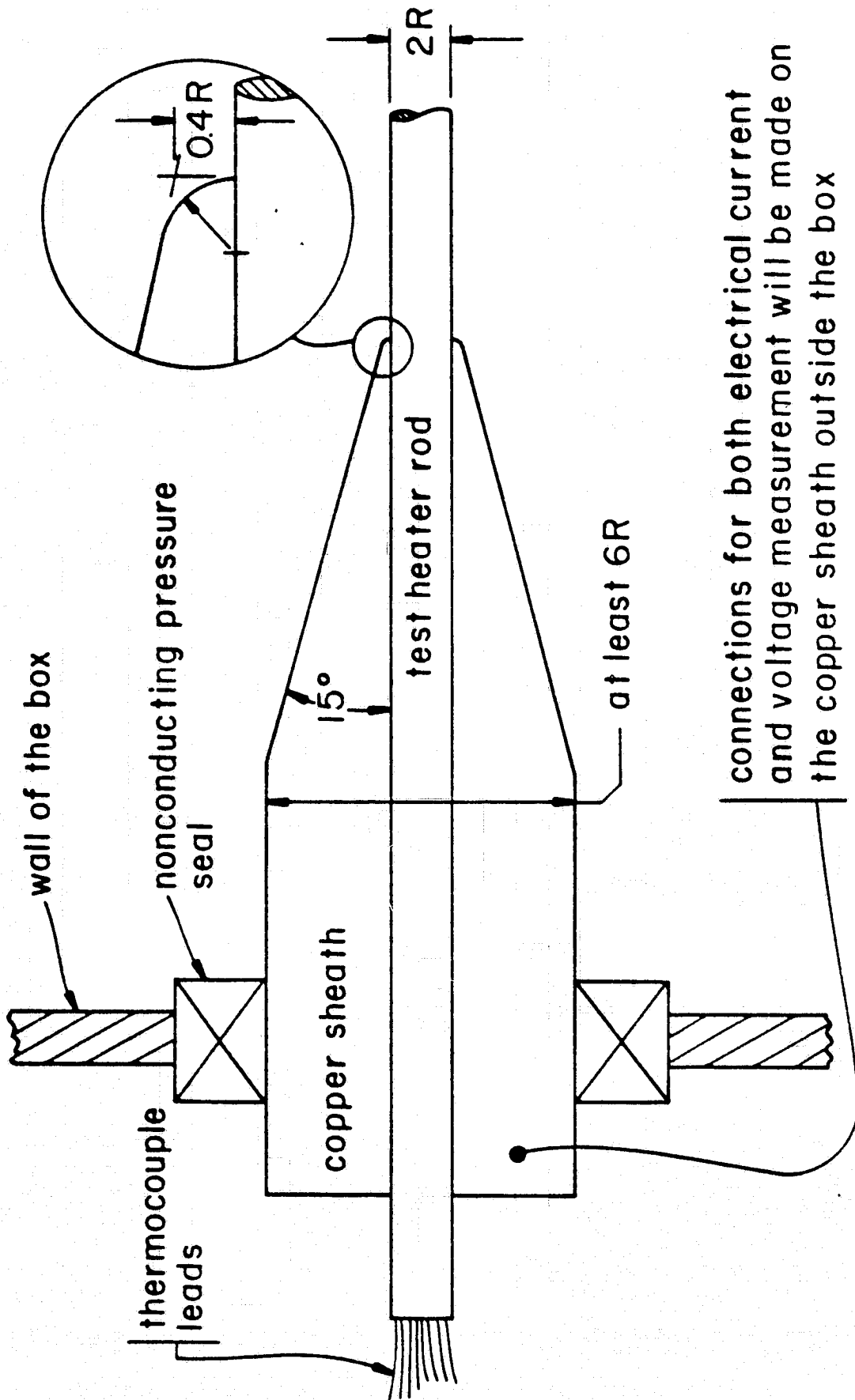


Fig. 6 Installation of the test heaters in the box

The heater power supply. Before specifying the heater power supply we must resolve the electrical load into voltages and amperages. This task is accomplished by determining the electrical resistance of the platinum heating element and the required power dissipation. The maximum power demand for each test condition corresponds to the film boiling heat flux at  $-500^{\circ}\text{C}$  in Figure 4. The detailed heater configuration and power requirements are summarized in Table 5.

Since the voltage demands of the system are low, and since D.C. is required, the current may be conveniently supplied by a small battery operating through a rheostat. The power supply for the small heaters should be provided by a conventional three-cell battery with about  $1\frac{1}{2}$  volts per cell. One to three of these cells is to be imposed in series according to the voltage required for the heater in question (see Table 5). If each of the twelve experiments were to be conducted twice for a period of about 45 seconds per run, the demand on the battery would be on the order of only 10 amp-hrs, so a single small battery should be adequate for the entire test.

The heating elements will be connected in series with a motor driven variable resistor that is programmed to ramp the heater current linearly from zero to maximum amperage during the test period. The heater power will be initiated when the test cell reaches the preheater set temperature and will be cut off when the heater temperature reaches  $-500^{\circ}\text{C}$  or when the elapsed time exceeds the allowable test period.



Table 5. Heater Size and Power Requirements

Condition No.	Heater dimensions				R at 500°C Ω	Q̇ watts	V volts	I amps
	O.D. (cm)	I.D. (cm)	Wall (cm)	Length (cm)				
1	.1524	.142	.0051	5.1	.0542	13.1	.843	15.5
2	.1524	.142	.0051	5.1	.0542	19.9	1.04	19.1
3	.0254	.01524	.0051	5.1	.393	6.3	1.57	4.0
4	.0254	.01524	.0051	5.1	.393	8.9	1.87	4.76
5	.635	.63	.00254	19.0	.094	117.8	3.33	35.4
6	.635	.63	.00254	19.0	.094	79.8	2.74	29.1
7	.17	.16	.0051	5.1	.0484	15.5	.87	17.8
8	.10	.089	.0051	5.1	.085	14.2	1.1	12.9
9	.061	.0508	.0051	5.1	.143	3.3	.687	4.8
10	.061	.0508	.0051	5.1	.143	4.9	.837	5.85
11	.61	.5842	.00254	19.0	.098	32.1	1.774	18.1
12	.61	.5842	.00254	19.0	.098	47.4	2.155	22.0

The circuit will be instrumented with voltage and amperage meters to continuously record the heater power.

The test cells. The test cell configuration is set on the basis of several constraints: The cross-section should be round on top and rectangular on the bottom to encourage the liquid to cling to the bottom under minimal gravity. It should be conceived with the notion that it will be 80 percent filled with liquid during operation. It should be wide enough to minimize sidewall effects and long enough to minimize end effects. Finally it should be fairly narrow with respect to its width.

Figure 7 shows the two test cells that we propose to satisfy these requirements. Certain dimensions and other features of these cells are set as follows: All of the small heaters are put in 8.18 cm long boxes, and the large ones are put in 25.05 cm long boxes. These lengths,  $\ell$ , will give sufficient aspect ratio to the heaters to avoid end effects. The height,  $h$ , is likewise specified as 5.1 cm and 12.1 cm respectively; and the width,  $w$ , is chosen between 1.27 cm and 3.81 cm, to give enough wall clearance without letting the boxes get heavy.

The boxes are to have pure copper walls which can be safely assembled with a good grade of soft solder since their temperatures remain low with respect to the softening temperatures of even the lowest grades of solder.

The windows of the test cells should be of a good optical quality plate glass, on the order of 1/2 cm in thickness. They should be mounted so as to give positive resistance to both imploding and exploding, as indicated in Figure 8. The heater and test cell

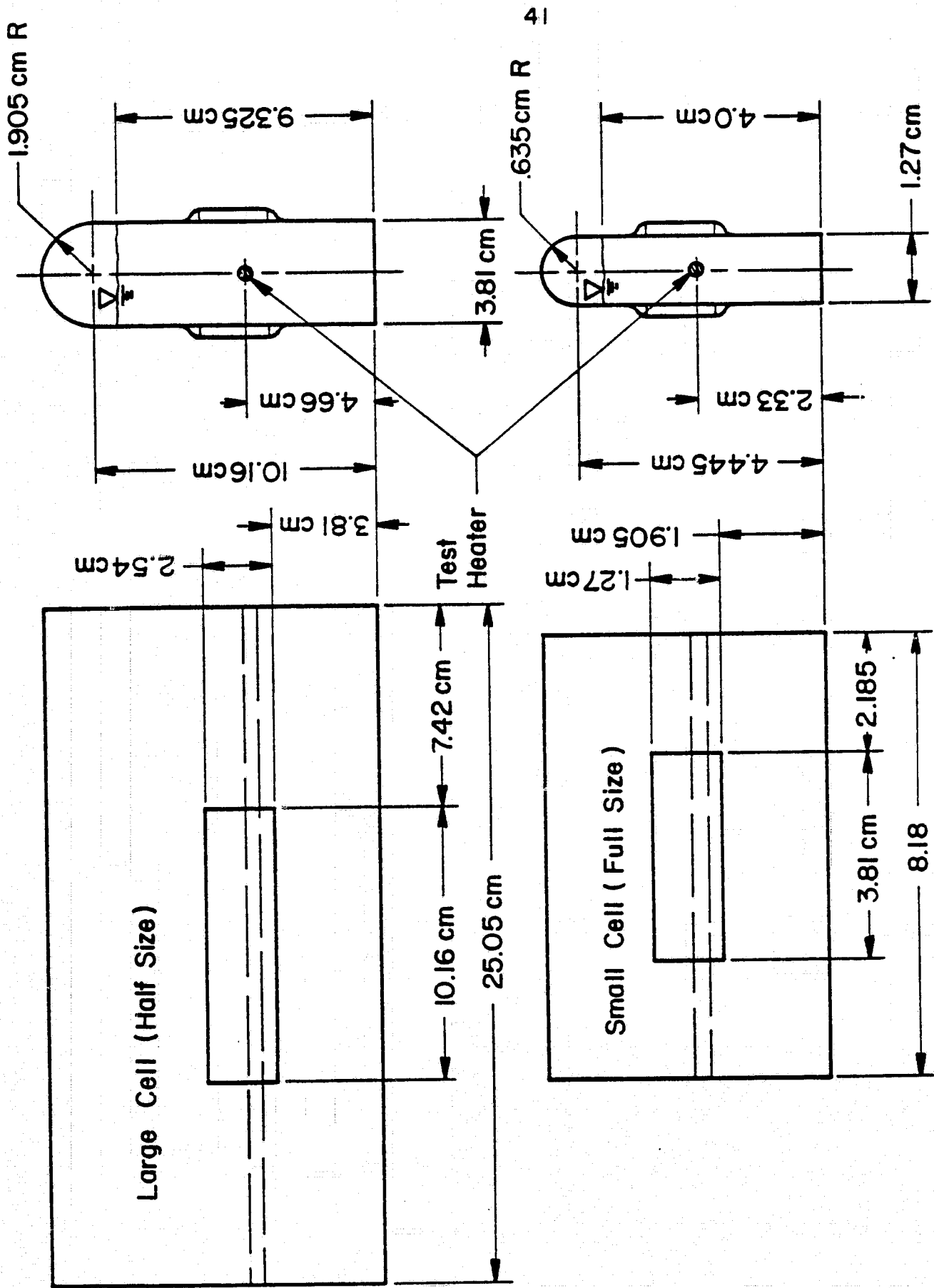


Fig. 7 Test Cell Configurations

specifications will now enable us to resolve the heat removal problem and to complete the preheater design.

The heat rejection problem. Figure 2 indicates that the scale parameter,  $R'$ , is insensitive to the cell pressure. Figure 3 shows that the flickering parameter,  $\Lambda$ , is more sensitive to pressure; and to learn more about its role we have suggested keeping the pressure somewhat above  $p_{\text{sat}}$  at room temperature, in each case. Since the exact operating pressure is not critical, we propose that no special care be taken to regulate the cell pressure closely. Instead we plan to let it drift a little with the temperature in the cell. Nevertheless, to assure that  $\Lambda$  is low enough to give useful information about the flickering phenomenon it will be necessary to assure that the temperature of the cell starts near the previously specified operating temperature and does not stray too far from it.

We calculate the temperature rise in each experimental test by presuming conservatively that the maximum heat flux is dissipated over the entire test duration in a volume of liquid, determined by the test cell dimensions. Since a 45 second test period was advantageous from the standpoint of the battery lifetime, we will stand by that figure for the temperature rise predictions.

(Ultimately it will turn out that a 45 sec run is consistent with motion picture camera limitations as well.) Table 6 summarizes the results of these calculations.

The twelve test conditions are described on the L.H.S. of Table 6. The liquid, the operating pressure,  $p_{\text{sat}}$  and the corresponding saturation temperature,  $T_{\text{sat}}$ , are listed first. The temperature difference  $\Delta T = T_{\text{sat}} - T_{\infty}$  (where the cabin temperature  $T_{\infty}$  is taken to be

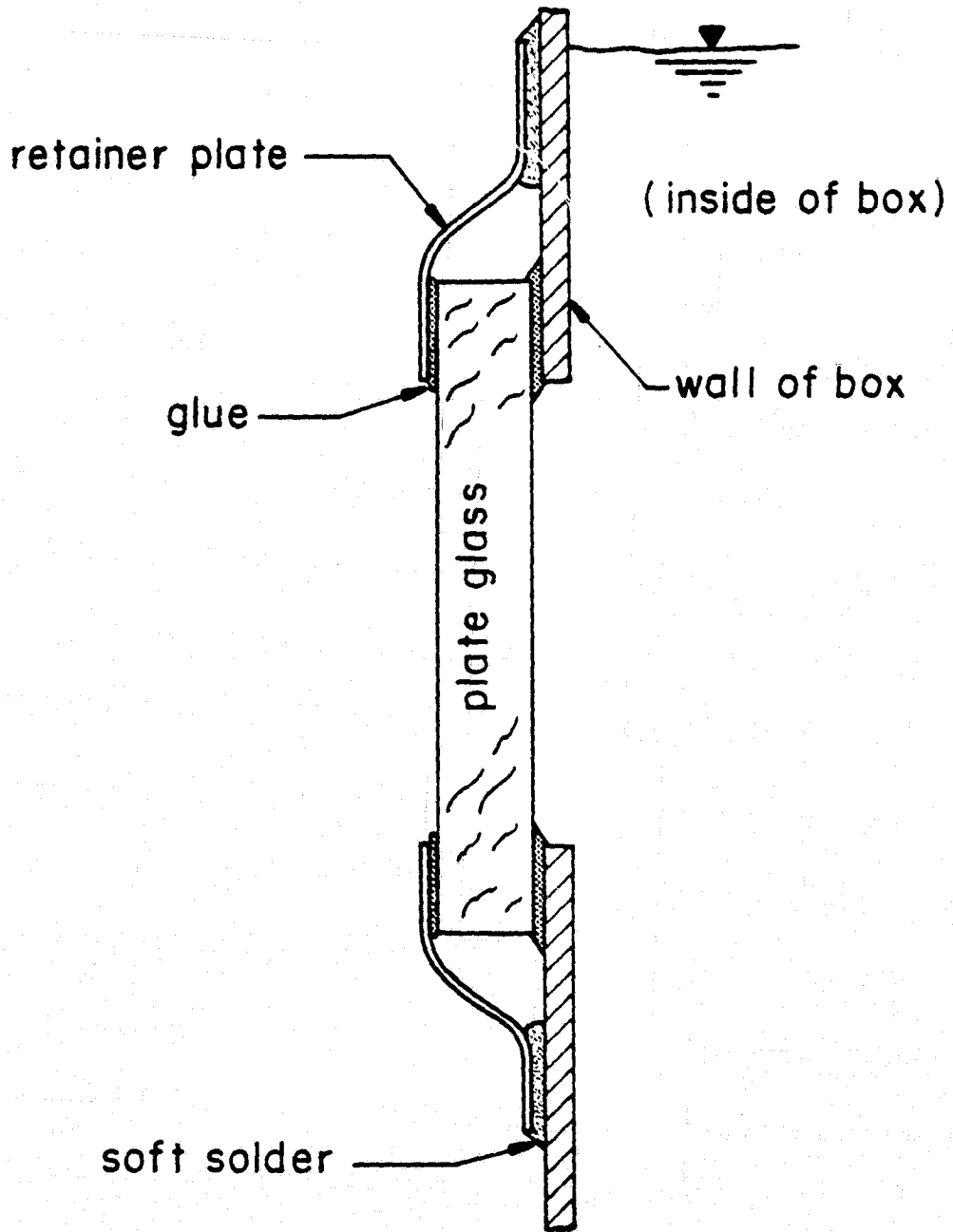


Fig. 8 Method of window retention

Table 6. Temperature Rise Calculation

CONDITION NUMBER	TEST CONDITIONS				CELL SIZE		MAXIMUM HEAT DISSIPATION $\dot{Q}$ (W)	TEMPERATURE RISE (°C)	
	liquid	P <sub>sat</sub> (atm)	T <sub>sat</sub> (°C)	$\Delta T$ (°C)	w (cm)	h (cm)			l (cm)
1	water	0.17	57	36	1.27	5.1	8.18	13.1	5.8
2	water	0.17	57	36	1.27	5.1	8.18	19.9	5.8
3	water	0.17	57	36	1.27	5.1	8.18	6.3	5.8
4	water	0.17	57	36	1.27	5.1	8.18	8.9	5.8
5	meth.	0.33	39	18	3.8	12.1	25.05	117.8	4.0
6	meth.	0.33	39	18	3.8	12.1	25.05	79.8	4.0
7	meth.	0.33	39	18	1.27	5.1	8.18	15.5	8.7
8	meth.	0.33	39	18	1.27	5.1	8.18	14.2	8.7
9	F-113	0.67	36	15	1.27	5.1	8.18	3.3	3.7
10	F-113	0.67	36	15	1.27	5.1	8.18	4.9	3.7
11	F-113	0.67	36	15	3.8	12.1	25.05	32.1	2.1
12	F-113	0.67	36	15	3.8	12.1	25.05	47.4	2.1

21°C) is also listed. The final cell dimensions, maximum heat fluxes, and the calculated temperature rise during a 45 second run are listed on the R.H.S.

The resulting liquid temperature rises are all small enough that they will not seriously alter the test condition. Thus we are safe making 45 second runs, and no external cooling of the test cell will be required.

The cell preheater. A preheater will be employed to condition the test cell internal environment to the prescribed temperature and pressure at the start of each experiment. The preheater will consist of an electrical resistance heating element fixed to the bottom of the test cell and powered by the 24 VDC spacelab power supply. The preheater will be turned full on or off by a thermostat which is controlled by a thermocouple located in the vapor region of the test cell.

A major constraint on the preheater operation is that the heat input to the cells must be very slow to avoid nucleation. The preheater will therefore be operated in two steps. First, the test cells will be placed in an insulated chamber and "warmed" to the desired saturation temperature. Second, the cells will be transferred to the test section and the preheater will be used to maintain the desired test conditions by supplying any heat that is lost to the cabin environment.

In the first step of the preheater operation, the test cells containing water will be kept in one chamber and heated to the 55-60°C temperature range. Another chamber will house the methanol and Freon filled test cells while they are being heated to the

35-40°C temperature range. The preheater resistance will be  $(24^2/w)\Omega$  so that each test cell will draw a specified number of watts,  $W$ , when it is matched to the 24 VDC electrical supply. Since the heat transfer will occur predominately by conduction, the test cells should be placed in close thermal contact inside the insulated chambers. A transient heat transfer analysis of the temperature rise of liquid in the cells indicates that the minimum warm up time of the largest cells will be on the order of one hour.

During the second step of the preconditioning operation involving the transfer of the cell from the chamber to the test stand, the preheater will again be powered. The power input,  $W$ , will be selected to match the radiation heat loss from the test cell to the cabin environment. The power requirements to maintain steady state conditions in the cell are summarized in Table 7.

The cell pressure. We have specified operating pressures for each of the test conditions and have stated that we will allow the cell pressure to vary with the temperature. Since the pressure may vary over a small range, pressure transducers will be inserted through the top of the test cells to enable continuous monitoring of the cell pressure. The transducers will also be coupled to pressure relief valves that will be set to open at 2 atm. The values should vent overboard -- probably through the forced convection experiment's venting system.

Preflight test cell preparation. Prior to the flight, each cell must be filled with its respective fluid, and four instrumentation elements must be sealed in. The following instrumentation elements should be located near the middle cross-sectional plane of the cell:

1. a vapor-phase thermocouple entering from the top of the box,



Table 7. Preheater Power Requirements

Condition Number	TEST CONDITION				$\Delta T$ (°C)	PREHEATER POWER $\dot{Q}_{in} = \dot{Q}_{rad}$ (W)
	liquid	$P_{sat}$ (atm)	$T_{sat}$ (°C)			
1	water	.17	57		36	2.2
2	water	.17	57		36	2.2
3	water	.17	57		36	2.2
4	water	.17	57		36	2.2
5	meth.	.33	39		18	6.1
6	meth.	.33	39		18	6.1
7	meth.	.33	39		18	1.0
8	meth.	.33	39		18	1.0
9	F-113	.67	36		15	0.8
10	F-113	.67	36		15	0.8
11	F-113	.67	36		15	5.0
12	F-113	.67	36		15	5.0

2. a liquid-phase thermocouple located between the heater and the bottom of the cell,
3. another liquid thermocouple located between the wall and the cylindrical heating element just out of the window view,
4. a combination pressure probe and pressure relief valve in the top of the test cell.

The last three items will be sealed in place before the box is filled. But the vapor-phase thermocouple will be held out since that port is to be used as a filling hole.

The box will then be heated to the normal boiling temperature of the liquid it is to contain. A tube will be inserted through the open port (with a little clearance) and directed into the bottom of the box. Saturated vapor will then be blown through the tube. Most of it will scavenge air from the box and some will condense. The liquid level in the box will be adjusted to that desired by controlling the inlet temperature of the vapor. The scavenging process will be permitted to proceed for an hour or so to remove almost all of the air. Then the top thermocouple will be inserted and the box will be permanently sealed.

#### F. Supporting Requirements

Environmental. No fewer than six, and no more than twelve, 45 sec bursts of elevated gravity ( $10^{-2}$  times earth-normal) will be required. These will be required for the six  $10^{-2} g_{\text{earth}}$  runs and zero to six replications of these runs. A  $10^{-4} g_{\text{earth}}$  environment will be required for the remaining six runs and zero to six replications of these runs.

Volume and Weight. Integration of the present experiment into the flow boiling experiment [18] should minimize space and weight requirements. A motion picture camera will be shared. We presume that about 114,000 frames, or 6,000 ft of movie film must be added to the existing magazine. The weight increase amounts to 34 kg.

Hardware for mounting this experiment should be minimal -- between one and ten kg. The test cells (depending upon whether it is decided to include backup units, and upon the details of the final design) should weigh between eight and 12 kg. Two warming boxes should weigh one to two kg and the battery about one kg. Other valving, instrumentation, and wiring should be light -- between one and five kg. The total weight should be somewhere between 46 and 64 kg with film being the major contributor. All payload items from this experiment should be returned to the earth.

Volume will also be minimal and we presume that the modest requirements can be fit into the two phase experiment space.

#### G. Procedure

The test cells should not be removed from their warming boxes prior to the tests. When an experiment is to be made the operator should:

1. load the camera and switch it to the pool boiling experimental circuit,
2. set the camera lens,
3. remove a test cell from the warming box and set it in its experimental rack. (He should tap it into place once or twice to get all of the test fluid in the "bottom".),
4. attach the "umbilical" cord containing the thermocouple, preheater, and power leads to the pool boiling experimental circuit

5. connect the overboard dump line to the safety valve,
6. take pencil and pad in hand to make any notes on visual observations during the test,
7. push the experiment activation button and watch closely as the experiment proceeds,
8. wait for ground-control to recommend on rerunning the experiment,
9. do a second run at the second gravity level, with any replications called for by ground control, and
10. disconnect the cell and return it to the warming box.

This process should take about 15 to 20 minutes for each of six test cells, with a reasonable number of replications (only a few of which will employ film). If the data acquisition is arranged to give immediate computer printout of the boiling curves, the decision to replicate can be made promptly.

#### H. Data Acquisition

The following items should be monitored continuously during each experimental run:

- 3 thermocouples recording cell temperatures
- 6 (or more) thermocouples recording heater temperatures
- 1 pressure transducer
- 1 voltage across the heater
- 1 amperage through the heater
- 1 accelerometer

The following events must be noted as a function of time during each test:

- The initiation of the camera

Any activation of:

- the pressure relief valve
- the electric power cutoff if it terminates a run before the maximum duration of 45 seconds has been reached.

The data acquisition system is designed to be extensively automated so that the operator will be free to record his own observations of the boiling process. The experiment control system and data acquisition system will be initiated simultaneously by one switch.

After battery power has been applied to the heaters, a two second time delay before starting the movie camera will permit a performance check of the other equipment to ensure that the experiment is operating properly.

Motion picture records of each run will be a very important component of the data acquisition process. The movies should be made with an appropriate high speed motion picture camera. We recommend that each run be sampled at about 200 frames per second with a 20 or 50-to-one shutter. This framing-rate is about as slow as it is possible to go without being in danger of missing events.\* Bakhru used a camera speed of 500 fps with a ten-to-one shutter and typically obtained pictures like that shown in Figure 9. By reducing the framing rate to 200 we reduce the information collected to 40 percent of that shown in Figure 9. That should be adequate and it will permit recording 38 seconds of each run on a 400 ft reel of film. This will fit nicely with the previously specified maximum duration of 45 seconds for any run.

---

\*A somewhat higher "minimum" value was suggested in Progress Report #6.

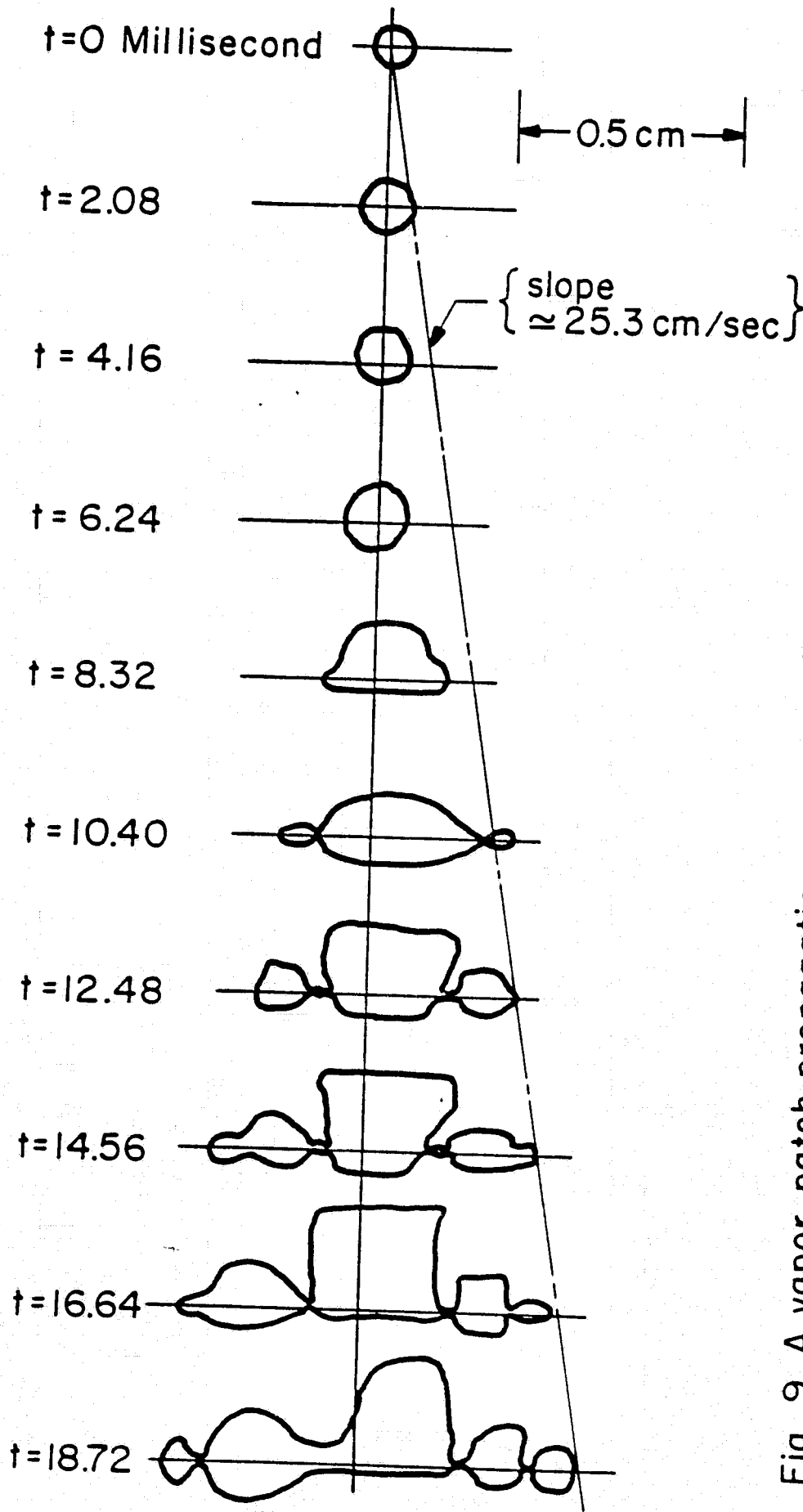


Fig. 9 A vapor patch propagation sequence illustrating propagation of a vapor front. 0.0254 mm pt. wire.  $R' = 0.16$ ,  $q = 520,506$  W/m<sup>2</sup> (After Bakhru)

Light should be directed into the camera through the subject, as shown in Figure 1, at an angle of  $10^{\circ}$  off the axis of the camera lens. It should be passed through a diffuser at the back window of the test cell. The light should be bright enough to permit an f-setting which will give a depth of field equal to most of the width of the cell. Each box should have an identifying symbol on a lower corner of the front window. It should be designed so that it will be clearly identifiable within the focus at that point.

#### I. Cost Analysis

The costs of the experiment can only be guessed very roughly and, we hope, without underestimating. Costs can be resolved into five categories: Design, Materials and Processes, Fabrication, Equipment, Preflight Testing, and Data Processing Software.

Design. Two months work by a designer and a detailer at \$25,000 and \$12,000 per year subject to 150 percent overhead. \$15,400

Materials and Processes. It will be necessary to experiment with the methodology for manufacturing the heaters. The only material cost that promises to be substantial will be the platinum. A very rough idea of costs is: \$ 5,000

Fabrication. Fabrication should require about two man-months at about \$18,000 per year with 150 percent overhead. \$ 7,500

Equipment. We presume that appropriate cameras are owned by NASA. Data acquisition systems already exist and need not be charged to this experiment. Batteries must be purchased, so too must other minor hardware connected with control. These items should come in below \$ 3,000

<u>Preflight Testing.</u> Two man-months of engineering time (\$4,000) and one man-month of technician's time (\$1,250) with 150 percent overhead.	\$13,000
<u>Data Processing Software.</u> An experienced programmer should be able to develop the software to deal with the data within two weeks time (\$1,000 with 150 percent overhead.)	\$ 2,500
Total estimated costs, less than	<u>\$46,500</u>

#### J. An Alternate Experimental Arrangement

The use of sealed cells introduces the concern that the cell pressure will be increased when boiling begins, whereupon simultaneous condensation might occur on the periphery of the bubbles. Such condensation could conceivably distort the the boiling process. We believe, although we are not certain, that the pressure rise should be modest, and condensation sufficiently slow, as to cause no serious distortion.

One way to circumvent this problem would be to maintain the cell pressure close to the design saturation pressure. This could be accomplished by providing a seal on each test cell which would be punctured just prior to the experimental run. The seal would be housed in such a way that the vapor is exposed to an appropriately sensitive and quick-acting pressure regulating valve leading to the overboard vent.

If this change were deemed necessary, the additional hardware would probably lead to modest increases in the cost and complexity of the proposed experiment. The change would also nullify reusing the cells and it would require means of dealing with the cells once they had been used.



REFERENCES

- [1] R. Siegel, "Effects of Reduced Gravity on Heat Transfer", Advances in Heat Transfer, Vol. 4 (J.F. Irvine Jr. and J.P. Hartnett, eds.) Academic Press Inc., New York 1967, pp 143-228.
- [2] C.P. Costello and J.M. Adams, "Burnout Heat Fluxes in Pool Boiling at High Accelerations", International Developments in Heat Transfer, ASME, N.Y. 1963, pp. 255-261. (This was the published account of a 1961 meeting which reported work done in the late 1950's).
- [3] N. Zuber, "Hydrodynamic Aspects of Boiling Heat Transfer," A.E.C. Report No. AECU-4439, Physics and Mathematics, 1959.
- [4] C.P. Costello and J.M. Adams, "The Interrelation of Geometry, Orientation, and Acceleration in the Peak Heat Flux Problem", Mech. Engr. Dept. Rept., Univ of Wash., Seattle, (ca. 1959).
- [5] J.H. Lienhard, "Interacting Effects of Geometry and Gravity Upon the Extreme Boiling Heat Fluxes", Jour. Heat Trans., Trans. ASME, Series C., Vol. 90, No. 1, 1968, pp. 180-2.
- [6] J.H. Lienhard, "Interacting Effects of Gravity and Size Upon the Peak and Minimum Pool Boiling Heat Fluxes", NASA CR-1551, May 1970.
- [7] J.H. Lienhard and V.K. Dhir, "Extended Hydrodynamic Theory of the Peak and Minimum Pool Boiling Heat Fluxes," NASA CR-2270, July 1973.
- [8] N. Bakhru and J.H. Lienhard, "Boiling from Small Cylinders," Int. J. Heat and Mass Transfer, Vol. 15, 1972, pp 2011-2025.
- [9] J.H. Lienhard and R. Bhatti; 2nd Monthly progress to NASA, Lewis Research Center; NASA Contract NAS3-20391, T. Cochran, Manager; May 1977, unpublished.
- [10] R.A. Reich and J.H. Lienhard, "A Computer Program for Correlating Peak and Minimum Heat Fluxes," Technical Report No. UKY 34-71-ME9, College of Engineering, University of Kentucky 1971.
- [11] Thermodynamic Properties of 'Freon' 113, Trichlorotrifluoroethane,  $\text{CCl}_2\text{F}-\text{CClF}_2$ , with Addition of Other Physical Properties," T-113A, E.I. Du Pont de Nemours and Company, Wilmington, Delaware, 19898, 1938.
- [12] R.C. Downing, "Transport Properties of 'Freon' Fluorocarbons, C-30," FREO, Technical Bulletin, E.I. Du Pont de Nemours and Co., 1967.
- [13] M. Alamgir and J.H. Lienhard, "The Temperature Dependence of Surface Tension of Pure Fluids," under review.
- [14] R.C. Reid and T.K. Sherwood, The Properties of Gases and Liquids, McGraw-Hill Book Company, N.Y., 1965, pp. 501-504.

- [15] S. Bretsznajder, Prediction of Transport and Other Physical Properties of Fluids, (Translated from the Polish by J. Bandrowski) Pergamon Press, N.Y. 1971, 295.
- [16] E.D. Washburn, International Critical Tables of Numerical Data, Physics, Chemistry and Technology, prepared by the National Research Council of the United States of America, Vol. III, McGraw-Hill Book Company, N.Y., 1928, p. 27.
- [17] J.H. Lienhard, "A Semi-Rational Nucleate Boiling Heat Flux Correlation", Int. J. Heat Mass Transfer, Vol. 6, 1963, pp. 215-219.
- [18] R.D. Bradshaw and C.D. King, "Conceptual Design for Spacelab Two-Phase Flow Experiments," NASA CR-135327, Dec. 1977.

APPENDIX A

Background Paper from

The International Journal of Heat and Mass Transfer,  
Vol. 15, 1972, pp 2011-25

# BOILING FROM SMALL CYLINDERS\*

NANIK BAKHRU

IBM Corporation, Hopewell Junction, New York 12533, U.S.A.

and

JOHN H. LIENHARD

Dept. of Mechanical Engineering, University of Kentucky, Lexington, Kentucky 40506, U.S.A.

(Received 27 September 1971)

**Abstract**—Heat transfer is observed as a function of temperature on small horizontal wires in water and four organic liquids. When the wire radius is sufficiently small, the hydrodynamic transitions in the boiling curve disappear and the curve becomes monotonic. Three modes of heat removal are identified for the monotonic curve and described analytically: a natural convection mode, a mixed film boiling and natural convection mode, and a pure film boiling mode. Nucleate boiling does not occur on the small wires.

The study was motivated by an interest in predicting the behavior of large heaters at low gravity. The application of the present results to such circumstances is therefore discussed. It is proposed that the peak and minimum heat fluxes will vanish at low gravity as well as on small wires.

## NOMENCLATURE

$Bi$ ,	Biot number, $hR/2k_w$ ;	$q_b$ ,	heat flux on the blanketed portion of the wire;
$f(R')$ ,	a function of $R'$ ;	$q_{max}, q_{min}$ ,	peak and minimum boiling heat fluxes, respectively;
$g$ ,	acceleration of a system in a force field;	$r$ ,	radius of a bubble;
$h$ ,	heat transfer coefficient, $q/\theta_w$ ;	$q_{max,F}$ ,	Zuber's predicted peak heat flux for a flat plate;
$h_{fg}$ ,	latent heat of vaporization;	$R$ ,	characteristic dimension, usually used to denote the radius of a cylindrical wire;
$h_{fg}^*$ ,	latent heat of evaporation plus 34 per cent of the sensible heat of vapor at heater wall;	$R'$ ,	dimensionless characteristic dimension (usually the radius), $R[g(\rho_f - \rho_g)/\sigma]^{1/2}$ ;
$k, k_g, k_w$ ,	thermal conductivity of liquid, vapor and heater, respectively;	$Ra^*$ ,	modified Rayleigh number, equation (16);
$Nu$ ,	Nusselt number, $2hR/k$	$T$ ,	temperature;
$Pe$ ,	dimensionless velocity, or Péclet number, defined by equation (8);	$T_w$ ,	heater surface temperature;
$p$ ,	pressure;	$\Delta T$ ,	wall superheat, $T_w - T_{sat}$ ;
$q$ ,	average heat flux on the entire heater. Also heat flux on the unblanketed portion of the heater when used with $q_b$ ;	$\Delta T_{ov}$ ,	temperature overshoot, $T$ at nucleation minus minimum $T$ for $q$ beyond nucleation;
		$t$ ,	time;
		$u$ ,	speed of vapor patch propagation;
		$v_{fg}$ ,	$(1/\rho_g) - (1/\rho_f)$ ;

\* This work was supported by NASA Grant NGR 18-001-035, under the cognizance of the NASA Lewis Research Center. The paper is extracted from the first author's doctoral dissertation at the University of Kentucky.

- $x, x_b$  axial distance coordinate: subscript  $b$  denotes reversed coordinate under the blanketed portion of the wire;
- $y$  distance measured from solid wall into liquid.

### Greek symbols

- $\alpha$  thermal diffusivity of heater;
- $A$  a dimensionless function.  
 $2\sigma h \nu_{f,q} T_{sat} \Delta T h_{f,q} k$
- $\mu$  viscosity of vapor;
- $\rho_f, \rho_g$  saturated liquid and vapor densities, respectively;
- $\sigma$  surface tension between a saturated liquid and its vapor;
- $\theta$  temperature measured above  $T_{sat}$ ;
- $\theta_m$  equilibrium temperature in the wire,  $q/h$ ;
- $\theta_0$  vapor patch triggering temperature;
- $\Theta, \Theta_0$  dimensionless temperatures,  $\theta/\theta_m$  and  $\theta_0/\theta_m$  respectively;
- $\xi, \xi_b$  dimensionless axial parameters defined after equation (10).

### General subscripts

- $b$  denoting conditions related to the portion of heater blanketed by vapor;
- $sat$  denoting conditions at saturation.

### INTRODUCTION

THE EARLY experiments of Nukiyama [1] and of Drew and Mueller [2] demonstrated that the plot of heat flux,  $q$ , against the liquid superheat at the heater surface,  $\Delta T$ , exhibited local maximum and minimum points. This discovery set the stage for a program of study that has lasted a third of a century. Since heat transfer is remarkably efficient near the local maximum, great effort has been directed toward predicting this limiting heat flux.

In 1948 Kutateladze [3] discussed the mechanism that dictated these extrema, and in 1958 Zuber (see e.g. [4]) provided an analytical

description of  $q_{max}$  and  $q_{min}$  for an infinite flat plate heater. For  $q_{max}$ , he found

$$q_{max} \approx \frac{\pi}{24} \rho_g^{\frac{1}{2}} h_{f,q}^{\frac{1}{2}} (\sigma g (\rho_f - \rho_g)). \quad (1)$$

The Zuber-Kutateladze theory says that  $q_{max}$  occurs when the vapor jets leaving the surface becomes Helmholtz unstable. It also says that the jets are arranged on a grid that is sized according to the Taylor unstable wavelength in the liquid-vapor interface. These instabilities arise as a consequence of inertial, interfacial, and buoyant forces.

The hydrodynamic theory has also been formulated for  $q_{max}$  in two finite geometries (cylinders [5] and spheres [6]) and for  $q_{min}$  on cylinders [7, 8]. For finite geometries it was shown independently by Bobrovich *et al.* [9] and by Lienhard and Watanabe [10] that if the characteristic dimension of a body is  $R$ , then

$$q_{max}, q_{max,F} = f(R') \quad \text{where}$$

$$R' = R \sqrt{[g(\rho_f - \rho_g)/\sigma]}. \quad (2)$$

Equation (2) has been shown [11] to apply as long as: the contact angle is small, the system is not close to the critical pressure, and the viscosity of the liquid is not great.

Under conditions of very low gravity, or for very small heaters,  $R'$  (which characterizes the ratio of buoyant forces to surface tension forces) becomes small. Figure 1 shows the  $q_{max}$  correlation, equation (2), as applied to about 900 horizontal cylinder data in [5]. In this case, an  $R'$  based on the radius,  $R$ , must exceed 0.15 if the Zuber-Kutateladze wave mechanisms which define  $q_{max}$  are to stay intact. For smaller values of  $R'$ , surface tension so over balances inertia that these mechanisms deteriorate, and a sampling of data by Kutateladze *et al.* [12], Sun and Lienhard [5], and Siegel and Howell [13] no longer correlate on  $q_{max}, q_{max,F}$  vs.  $R'$  coordinates.

It was likewise shown in [8] that there is still good visual evidence of the wave stability mechanisms for all  $R' \geq 0.12$ , during film

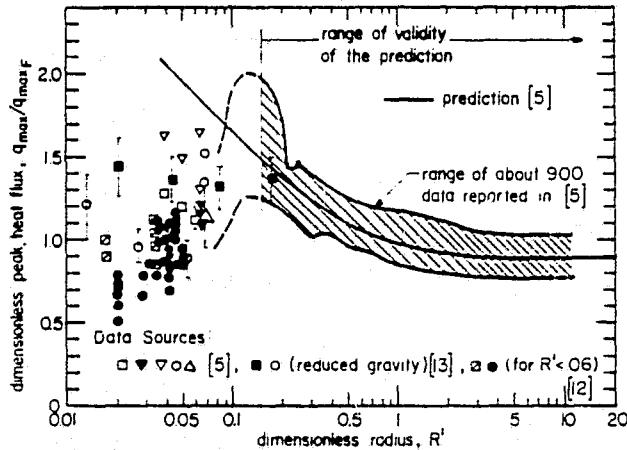


FIG. 1. Deterioration of  $q_{max}$  correlation at small  $R'$ .

boiling on horizontal cylinders. But for  $R' \leq 0.06$  these mechanisms cease to be identifiable.

If equation (2) fails, and the Zuber-Kutateladze mechanism fails with it, what exactly happens to the boiling process at small  $R'$ ? The photographs of Sun [5], of Pitts and Leppert [14], and of Kutateladze *et al.* [12] for small wires provide some clue. Bubbles grow on the wire until they are large enough to buoy off and there is no evidence of the inertial waves that are apparent on large wires. The photographs of Siegel and Usiskin [15] and Siegel and Howell [13] show the same kind of process

for greatly reduced gravity. The forces of surface tension and buoyancy remain important, however the process is slowed down and the effects of inertia are greatly reduced. Indeed, the soundtrack of a movie by Siegel and Keshock (associated with [16]) specifically notes the reduced inertia effects in boiling under low gravity.

The problem that we face is then this: "If, at low gravity or for small wires, inertia becomes insignificant and the Zuber-Kutateladze mechanisms fail, what replaces them?" We must now ask what the various investigators who

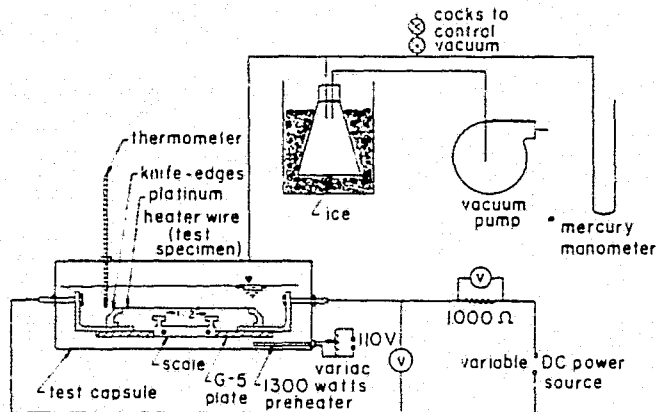


FIG. 2. Schematic representation of experimental apparatus.

have given  $q_{\max}$  and  $q_{\min}$  data for low  $R'$  have actually observed. Without the inertial wave mechanisms it is hard to see how there could have been any  $q_{\max}$  or  $q_{\min}$  points to report.

#### EXPERIMENT

To answer the question raised in the Introduction we set out to measure the full  $q$  vs.  $\Delta T$  curve for very small wires heating a variety of liquids. The apparatus used to do this is shown in Fig. 2.

A small platinum wire, which serves as both a resistance heater and a resistance thermometer, is suspended in the liquid of interest and boiling is observed at successive heat fluxes. The temperature of the wire was calculated from the resistance which in turn was computed from the ratio of voltage to current, using the method detailed by van Stralen and Sluyter [17]. Since complete details of the experimental method are given by Bakhru [18], we shall only list a few major features of the tests here:

The wires were cleaned in soap and then rinsed in the test liquid. Reagent grade liquids were used in all cases. During actual observations the preheater, which was used to maintain

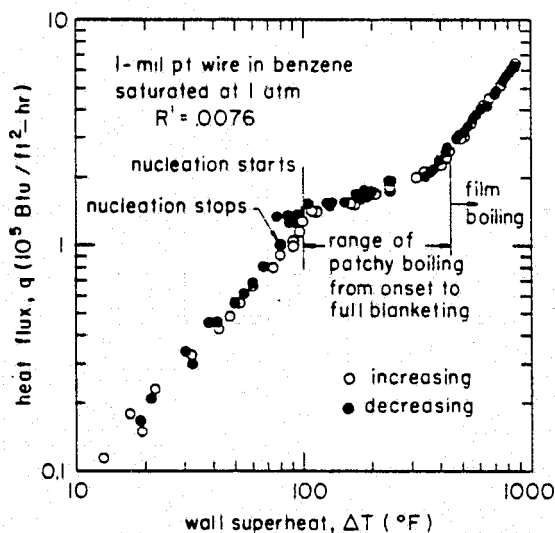


FIG. 3. Boiling curve for 1-mil platinum wire in benzene.

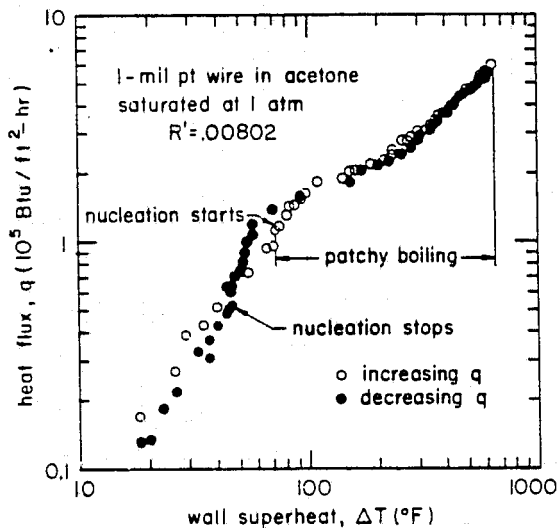


FIG. 4. Boiling curve for 1-mil platinum wire in acetone.

saturation conditions, was momentarily switched off. Since the wires would melt during atmospheric pressure runs in water, the water runs were all made at pressures in the neighborhood of 3 in. Hg abs. The maximum probable error in  $q$  was found to be  $2\frac{1}{2}$  per cent. The maximum probable error in  $\Delta T$  varied from

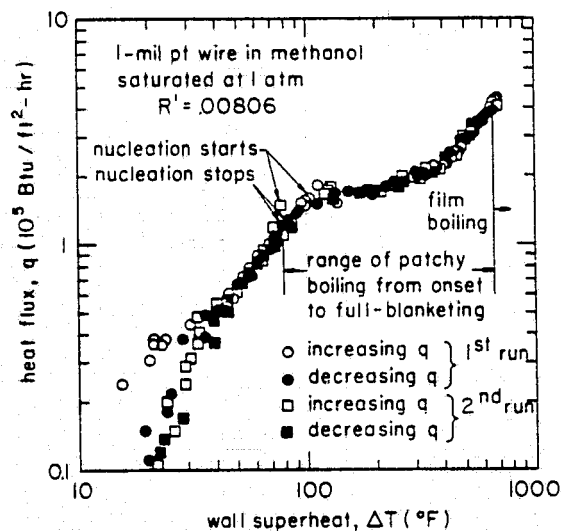


FIG. 5. Boiling curve for 1-mil platinum wire in methanol.

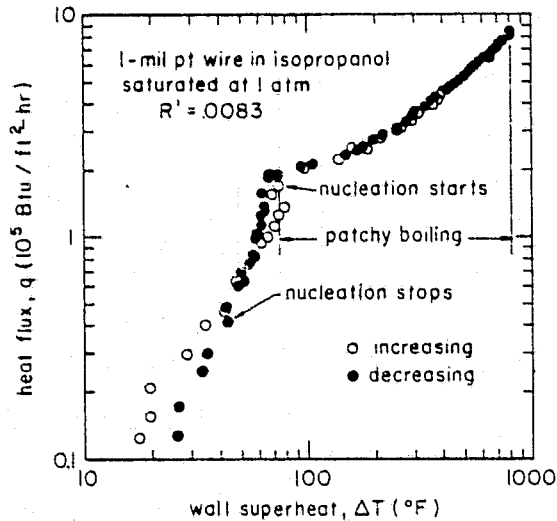


FIG. 6. Boiling curve for 1-mil platinum wire in isopropanol.

36 per cent or about  $5\frac{1}{2}$  °F at the very lowest  $\Delta T$ 's to 1.8 per cent or about 13 °F at the highest  $\Delta T$ 's.

Our complete raw data are given in the form of 13 boiling curves in Figs. 3-14. These have been arranged in order of increasing  $R'$  from 0.0076 up to 0.0806. In each case data are presented for both increasing and decreasing

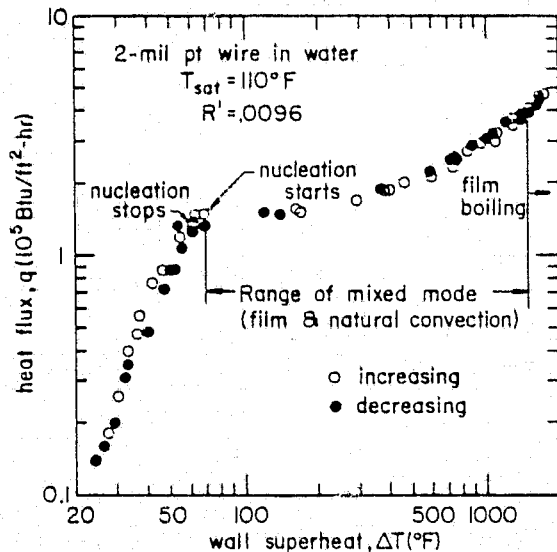


FIG. 7. Boiling curve for 2-mil platinum wire in water.

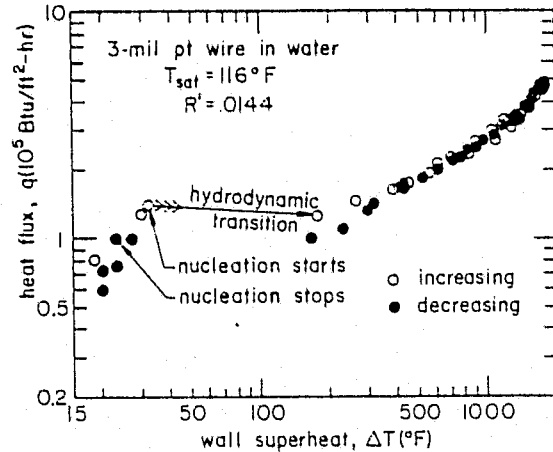


FIG. 8. Boiling curve for 3-mil platinum wire in water.

heat flux to expose any hysteresis effects. Figure 5 combines data for two wires under identical conditions to assure reproducibility of results.

The major significance of the present study is readily apparent from these curves. As  $\Delta T$  is increased on the smaller wires,  $q$  rises monotonically without passing through a maximum and minimum. Only as  $R'$  increases to about

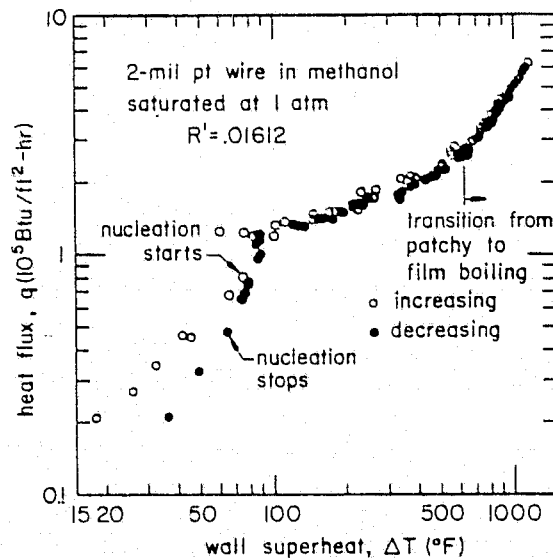


FIG. 9. Boiling curve for 2-mil platinum wire in methanol.